The Plant Cell, Vol. 24: 3725–3741, September 2012, www.plantcell.org

Plastid Localization of the Key Carotenoid Enzyme Phytoene Synthase Is Altered by Isozyme, Allelic Variation, and Activity[W]

Maria Shumskaya,[a] Louis M.T. Bradbury,[a] Regina R. Monaco,[a] and Eleanore T. Wurtzel[a,b,1]

[a] Department of Biological Sciences, Lehman College, City University of New York, Bronx, New York, 10468
[b] Graduate School and University Center, City University of New York, New York, New York 10016-4309

Plant carotenoids have unique physiological roles related to specific plastid suborganellar locations. Carotenoid metabolic engineering could enhance plant adaptation to climate change and improve food security and nutritional value. However, lack of fundamental knowledge on carotenoid pathway localization limits targeted engineering. Phytoene synthase (PSY), a major rate-controlling carotenoid enzyme, is represented by multiple isozymes residing at unknown plastid sites. In maize (*Zea mays*), the three isozymes were transiently expressed and found either in plastoglobuli or in stroma and thylakoid membranes. PSY1, with one to two residue modifications of naturally occurring functional variants, exhibited altered localization, associated with distorted plastid shape and formation of a fibril phenotype. Mutating the active site of the enzyme reversed this phenotype. Discovery of differential PSY locations, linked with activity and isozyme type, advances the engineering potential for modifying carotenoid biosynthesis.

INTRODUCTION

Carotenoids are a large class of yellow, orange, and red lipophilic molecules synthesized by all photosynthetic organisms (Cuttriss et al., 2011), aphids (Moran and Jarvik, 2010), and various bacteria and fungi (Velayos et al., 2000; Iniesta et al., 2008). In plants, carotenoids play multiple roles, such as photosynthetic light harvesting and protection against light and heat stress (Dall'Osto et al., 2007), and as precursors to hormones that mediate stress and developmental signaling (Auldridge et al., 2006; Messing et al., 2010; Walter et al., 2010). Carotenoid antioxidants increase heat and light stress tolerance by protecting membranes from reactive oxygen species and lipid peroxidation (Davison et al., 2002; Havaux et al., 2007; Johnson et al., 2007; Li et al., 2008b). Concentrated in fibrillar plastoglobuli of fruit chromoplasts (Egea et al., 2010), carotenoids provide color to attract animals that serve as plant seed distributors. Certain carotenoids in the endosperm tissue provide nutritional value and have been targets for improvement, especially in cereal crops of the grass family (Harjes et al., 2008; Vallabhaneni et al., 2009; Vallabhaneni and Wurtzel, 2009; Yan et al., 2010; Wurtzel et al., 2012).

The carotenoid biosynthetic pathway occurs in plastids where the lipophilic carotenoids accumulate in envelope/thylakoid membranes and plastoglobuli (Jeffrey et al., 1974; Siefermann-Harms, 1978; reviewed in Austin et al., 2006). Carotenoids are synthesized in both light- and dark-grown tissues, such as leaves, endosperm, and roots. In the dark, leaf tissues develop etioplasts with rudimentary prolamellar bodies, which are the precursors for thylakoids and support low levels of carotenoid biosynthesis (Welsch et al., 2000). In the light, leaves turn green due to development of highly specialized chloroplasts filled with complex photosynthetic systems. Carotenoids are distributed differently in etioplasts and chloroplasts; this distribution might also require differential localization of their biosynthetic enzymes. Phytoene synthase (PSY) catalyzes the committed step to carotenoid biosynthesis and is a key target for pathway engineering (Cuttriss et al., 2011). There are up to three PSY isozymes in evolutionarily distant plants, including all the major food staples in the grasses and other crops of agronomic importance (Gallagher et al., 2004; Pozniak et al., 2007; Fernandez et al., 2008; Giorio et al., 2008; Li et al., 2008a; Crawford et al., 2011; Qin et al., 2011; Rodríguez-Suárez et al., 2011; Xu et al., 2011; Tomato Genome Consortium, 2012). Different PSY isozymes mediate carotenogenesis in particular tissues, in response to developmental and physiological signals (for example, Li et al., 2008a, 2008b, 2009). Also, allele-specific variation accounts for yellow endosperm maize (*Zea mays*) and yellow-rooted cassava (*Manihot esculenta*) (Gallagher et al., 2004; Arango et al., 2010).

The core carotenoid biosynthetic pathway consists of ~10 enzymes (Cuttriss et al., 2011). However, the location of the biosynthetic pathway as a complete entity for controlling the unique spatial distribution of carotenoids remains unclear. Moreover, this pathway must respond to environmental and developmental signals to link photomorphogenesis, photoprotection, and stress responses with location-specific carotenoid synthesis and degradation. What is the nature of this dynamic pathway landscape and how do isozymes and allelic variants fit into the picture?

According to recent proteomic studies on *Arabidopsis thaliana* chloroplasts (Joyard et al., 2009; Ferro et al., 2010), many of the carotenoid biosynthetic pathway enzymes are exclusively localized to envelope membranes. Only a few carotenoid enzymes are found in thylakoids; these enzymes include xanthophyll cycle enzymes and phytoene desaturase (PDS). In pepper (*Capsicum*

[1] Address correspondence to wurtzel@lehman.cuny.edu.
The author responsible for distribution of materials integral to the findings presented in this article in accordance with the policy described in the Instructions for Authors (www.plantcell.org) is: Eleanore T. Wurtzel (wurtzel@lehman.cuny.edu).
[W] Online version contains Web-only data.
www.plantcell.org/cgi/doi/10.1105/tpc.112.104174

annuum) fruit chromoplasts, most carotenoid enzymes are localized to plastoglobuli (Austin et al., 2006; Ytterberg et al., 2006). In maize (*Zea mays*) proteomic studies, the only carotenoid enzymes detected were PDS and ζ-carotene desaturase that were found in membrane fractions of bundle sheath and mesophyll cells, respectively (Friso et al., 2010). Carotenoids are found in both cell types, yet other carotenoid biosynthetic enzymes were undetectable. Chloroplast suborganellar localization of the key pathway enzyme, PSY, has yet to be detected by proteomic analysis.

In this study, we investigated localization of PSY isozymes and allelic variants from maize, rice (*Oryza sativa*), and *Arabidopsis*. We find that PSY isozymes differ in chloroplast suborganellar localization and that overexpression of naturally occurring allelic variants produced striking differences in localization and profound effects on chloroplast architecture.

RESULTS

PSY Isozymes Exhibited Differential Localization in Maize Chloroplasts

To investigate localization of PSY isozymes, we chose PSYs from two cereal crops, maize and rice, and the model plant *Arabidopsis*. Both maize and rice have three PSY isozymes, and we tested Zm-PSY1, Zm-PSY2, Zm-PSY3 of *Z. mays* var B73; Os-PSY1 and Os-PSY2 of *O. sativa* var IR36 (Indica); and Os-PSY3 of *O. sativa* var TP309. Maize variety B73 has yellow colored kernels due to carotenoid accumulation in the endosperm mediated by Zm-PSY1 activity encoded by the maize *yellow1* (*y1*) locus. Rice does not accumulate endosperm carotenoids (Gallagher et al., 2004). *Arabidopsis* has only one At-PSY.

The localization of PSYs was studied by transient expression of fluorescent protein fusions in plant leaf protoplasts. Protoplasts retain their tissue specificity after isolation (Faraco et al., 2011; Denecke et al., 2012), thereby reflecting in vivo conditions, allowing us to observe localization of transiently expressed PSY proteins. This approach provides a great advantage for studying PSY, a low abundance protein that otherwise escapes detection in proteomic studies. Protoplast sources were chosen in consideration of different stages of plastid development. We isolated protoplasts both from dark-grown tissues (etiolated protoplasts) or light-grown tissues (green protoplasts). Also, we chose monocot maize leaves as a protoplast source for expression of PSYs from monocotyledonous species of maize and rice and dicot species of cowpeas (*Vigna unguiculata* subsp *unguiculata*) for experiments on PSY from dicotyledonous *Arabidopsis*. Each PSY protein together with its chloroplast target peptide was C-terminally fused to synthetic green fluorescent protein (sGFP) or red fluorescent protein (RFP), and transient expression was monitored by confocal microscopy. To confirm reliability of the approach, we tested proteins of known localization using protoplasts prepared from etiolated maize leaves (see Supplemental Figure 1 online).

We found that most, but not all, PSYs of all species studied were distributed in plastids the same way in both etiolated protoplasts (Figure 1A) and green protoplasts (Figure 1B), whether from monocots or dicots. These PSYs localized to chloroplasts in specific fixed speckles, distributed inside the plastid and attached to areas that displayed red chlorophyll fluorescence indicative of prolamellar bodies or thylakoids. The size and distribution of the speckles were suggestive of plastoglobuli: Spherical lipid structures attached to thylakoid membranes of chloroplasts or distributed in chromoplast stroma (Steinmüller and Tevini, 1985). To define the nature of the speckles, we performed a transient expression assay with a protein from the fibrillin family, since fibrillins are structural proteins of plastoglobuli (Singh and McNellis, 2011). We identified maize plastoglobulin-2 (Zm-PG2) by BLAST search as a homolog to several fibrillins from *Arabidopsis* (AT4G04020, AT4G22240, and AT2G35490, 80 to 90% sequence similarity). Zm-PG2 has a PAP-fibrillin domain and is also homologous to the other *Arabidopsis* fibrillins of the superfamily (50 to 60% similarity). The isoelectric point (5.4) and hydrophobicity (GRAVY index, −0.142) of Zm-PG2 were similar to *Arabidopsis* fibrillin FBN4, which is a core protein of plastoglobuli (Lundquist et al., 2012), although minor amounts of FBN4 are also identified by proteomic studies in chloroplast stroma. Zm-PG2 was fused to RFP and expressed in cowpea and maize protoplasts (Figure 2A). Indeed, in cowpea and maize green tissue protoplasts, the speckled pattern of Zm-PG2-RFP was identical to the speckled pattern of the majority of PSYs. However, in etioplasts, Zm-PG2-RFP was distributed evenly throughout, suggesting a stromal localization for this fibrillin in dark-grown tissue. We also coexpressed Zm-PSY2-GFP and Zm-PSY3-GFP along with Zm-PG2-RFP in green protoplasts (Figure 2B). The GFP signal of the PSYs was distributed in speckles together with the RFP signal of Zm-PG2. Merging of both signals confirmed colocalization of PSYs with Zm-PG2; thus, we consider the speckles to be plastoglobuli.

Zm-PSY1-GFP stood alone from the group of other PSYs. In etioplasts, Zm-PSY1-GFP was distributed throughout, together with small bright (punctate) spots attached to membranes of red fluorescent prolamellar bodies, very different in appearance from plastoglobuli in the case of all other PSYs. Homogeneous filling of plastids indicated a soluble, stromal location of Zm-PSY1. In light-grown tissue, Zm-PSY1-GFP was evenly distributed throughout the chloroplast. In chloroplasts, the association with membranes could not be seen but should not be excluded due to limitations of image resolution.

Import Experiments Confirmed Peripheral Membrane Binding of Chloroplast-Localized PSYs

We discovered using transient expression that Zm-PSY2 and Zm-PSY3, as well as rice and *Arabidopsis* PSYs, localized to plastoglobuli, structures mostly attached to the surface of thylakoid membranes. Therefore, PSYs were expected to associate with lipids/membranes. To confirm this hypothesis, we tested the three maize PSY isozymes by chloroplast import assay. In vitro–translated ^{35}S-labeled Zm-PSY precursor proteins were imported into isolated pea (*Pisum sativum*) chloroplasts, followed by chloroplast fractionation into three parts: soluble, membrane, and alkaline-treated membrane (to purify from peripherally bound proteins) (Figure 3). After import, chloroplasts were treated with thermolysin to remove unimported proteins. The unimported protein, seen in the import samples of Zm-PSY2 and Zm-PSY3 as an upper band, completely disappeared after

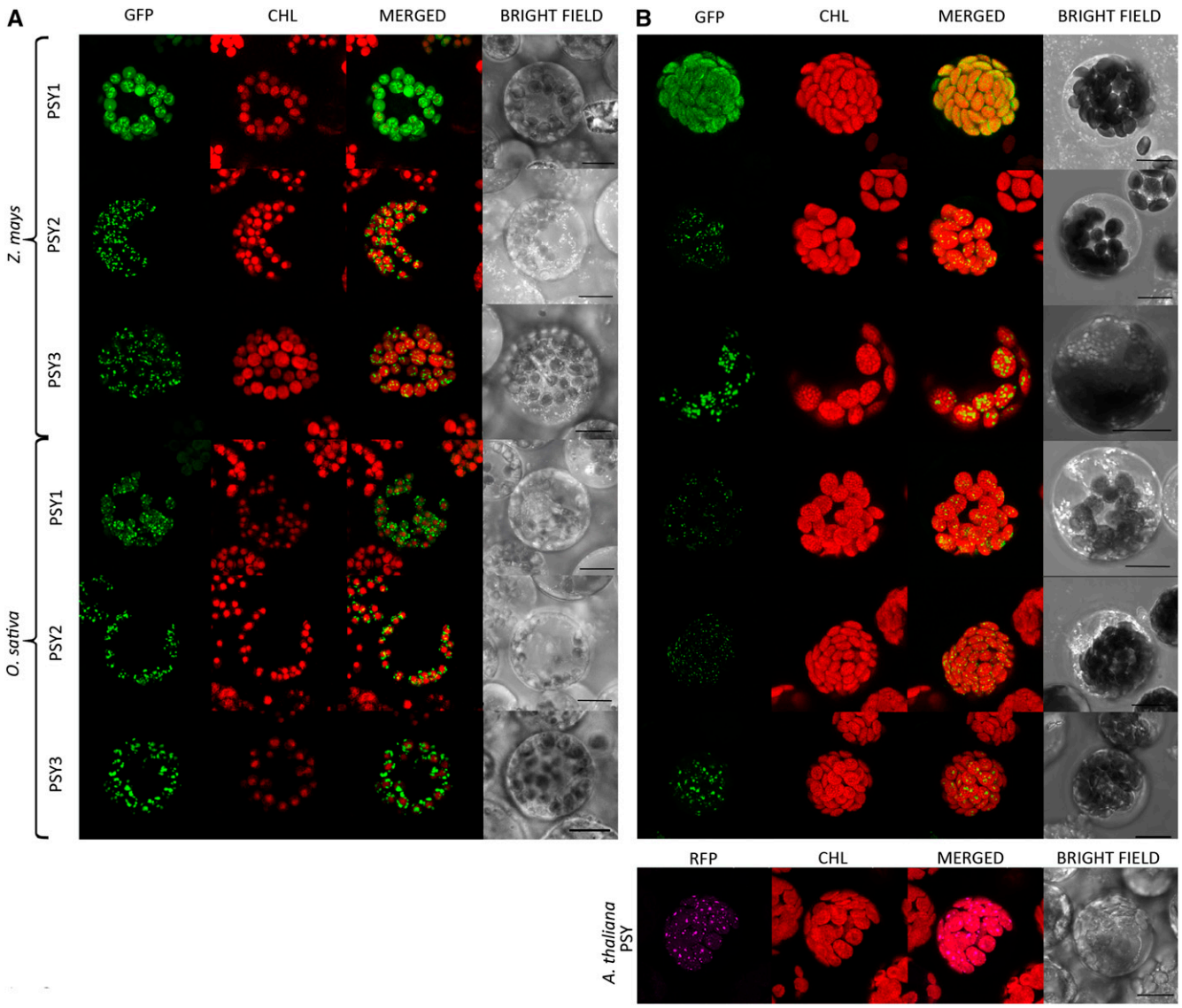

Figure 1. Transient Expression of Various PSY-GFP Fusion Constructs in Leaf Mesophyll Protoplasts.

(A) Expression in etiolated maize protoplasts. All PSYs from maize and rice, except Zm-PSY1, are localized to specific speckles. Zm-PSY1 is localized to stroma and associated to prolamellar bodies. CHL, chlorophyll autofluorescence, concentrated in a partial area of an etioplast.

(B) Expression of Zm-PSYs and Os-PSYs in green maize protoplasts and of At-PSY-RFP in green cowpea protoplasts. All PSY from maize, rice, and *Arabidopsis*, except Zm-PSY1, are localized to specific speckles. Zm-PSY1 is localized to stroma. CHL, chlorophyll autofluorescence, occupying the entire area of a chloroplast.

Bars = 10 μm.

thermolysin treatment, and only the imported mature protein remained, being protected by the envelope membrane (Figure 3B, arrow). Fractionation of these chloroplasts revealed that Zm-PSY2 and Zm-PSY3 were peripherally bound to chloroplast membranes. These results are consistent with association of these proteins with plastoglobuli, as was suggested by transient expression in protoplasts.

The results of chloroplast import of Zm-PSY2 and Zm-PSY3 were similar to Os-PSYs (Welsch et al., 2008). In import experiments with pea chloroplasts, Os-PSYs are known to be associated with the membrane fraction (although alkaline treatment of the membrane fraction was not performed, the lack of integral membrane helices in the reported structural predictions of Os-PSYs suggested that they were likely to be peripherally bound).

Compared with other PSYs, Zm-PSY1 from yellow endosperm maize behaved uniquely in the import experiments, just as we found for Zm-PSY1 localization in protoplasts. After thermolysin treatment, the envelope-associated precursor band disappeared as expected, leaving an undigested band of a mature protein ~42 kD (Figure 3B, arrow). However, a smaller band ~20 kD appeared

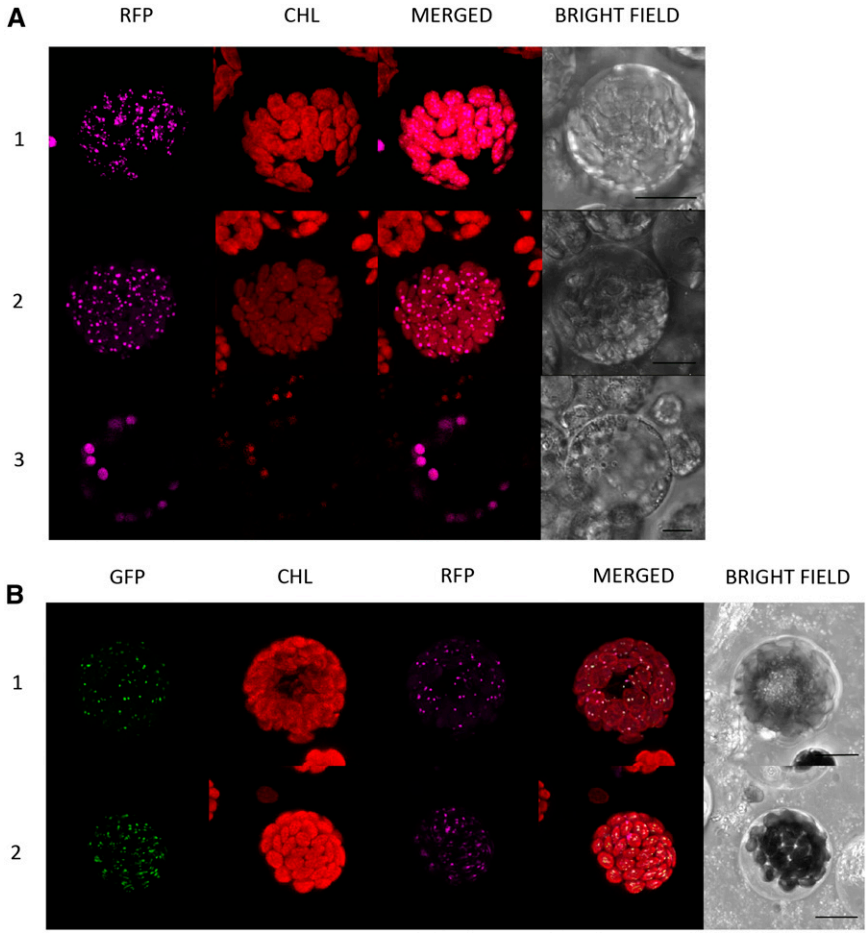

Figure 2. Plastoglobuli Localization of Various Proteins in Mesophyll Protoplasts.

(A) Transient expression of Zm-PG2-RFP, suggesting localization to plastoglobuli. 1, Expression in cowpea cotyledon protoplasts. 2, Expression in green maize protoplasts. 3, Expression in etiolated maize protoplasts. 1 and 2 show plastoglobular localization, and 3 shows stromal localization.
(B) Transient coexpression of Zm-PSY2-GFP (1) and Zm-PSY3-GFP (2) with Zm-PG2-RFP. Zm-PSYs and Zm-PG2 are colocalized, as seen on merged image, indicating plastoglobular localization of Zm-PSY2 and Zm-PSY3.
CHL, chlorophyll autofluorescence. Bars = 10 μm.

(Figure 3B, star). This smaller peptide might be a part of Zm-PSY1 that is located within the membrane and therefore is protected from protease treatment. The pattern after the thermolysin treatment looked similar to one of the integral proteins from the outer chloroplast membrane, Toc34. The intermembrane and periplasm facing domains of Toc34 remained untouched by thermolysin. Fractionation of chloroplasts showed that Zm-PSY1 is peripherally associated with membranes as found for the other PSYs.

Altogether, the results suggested that Zm-PSY1 was somehow localized to chloroplasts in two forms. One form of Zm-PSY1 is bound to the envelope membrane. A second form of Zm-PSY1 is peripherally bound to thylakoids. The peripheral membrane association of Zm-PSY1 agrees with the results of transient expression in etiolated protoplasts, where punctate spots of Zm-PSY1-GFP were observed around prolamellar bodies.

Single Amino Acid Variants Displayed Altered PSY1 Localization and Transformed Plastid Architecture

Transient expression and import experiments suggested that almost all investigated PSYs were localized to plastoglobuli, regardless of whether the plants were grown in light or dark. Zm-PSY1 was unique and exhibited dual localization to stroma and attached to membranes, as clearly seen in etioplasts (Figure 1). Our next step was to identify protein features responsible for differences in localization. We aligned PSYs (Figure 4) and searched for amino acids that are shared by all PSYs except for Zm-PSY1 from yellow endosperm maize. A striking difference was found in the highly conserved coding region, at amino acid residue 257, which was a Thr (Thr-257) in Zm-PSY1 compared with Pro in other PSYs. Another position, 168, was occupied by Asn in Zm-PSY1 (Asn-168), in contrast with Ser in all other PSYs. BLAST alignment of Zm-PSY1 from yellow endosperm

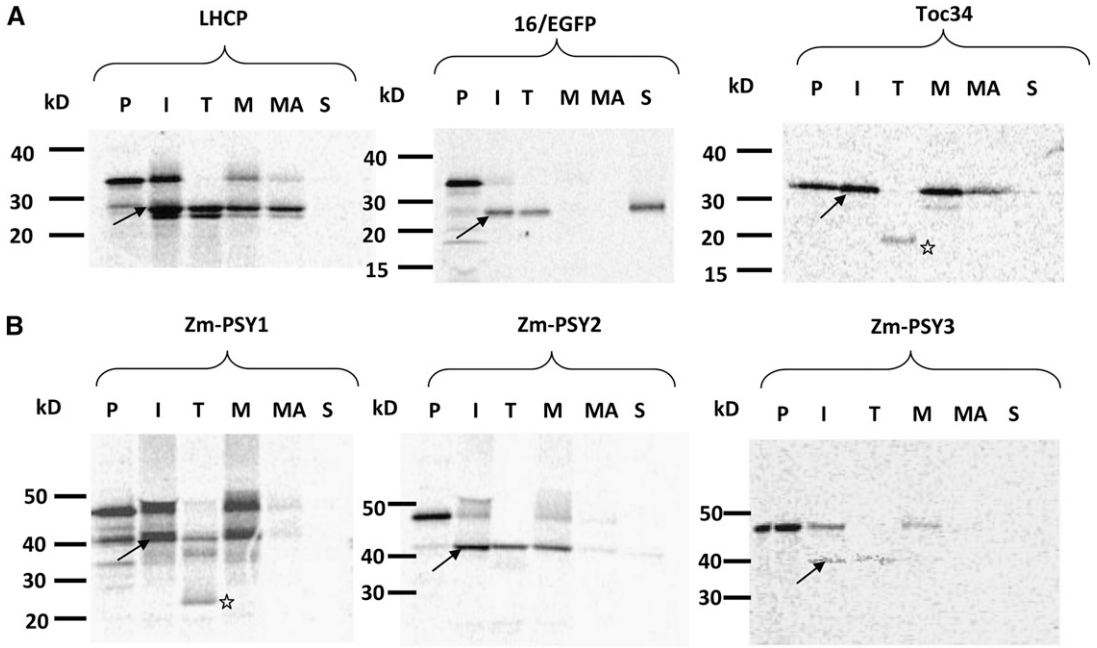

Figure 3. Import of Proteins into Chloroplasts.

Protein precursors were made by in vitro transcription/translation. Protein precursors were incubated with isolated chloroplasts for import and processing to the mature forms. Mature proteins were resistant to thermolysin treatment of chloroplasts after import and of smaller mass compared with the unimported precursors. kD, molecular mass marker; I, import of radiolabeled precursor protein into intact chloroplasts; M, membrane fraction; MA, purified membrane fraction (after alkaline treatment); P, precursor (1 μL of the translation mix); S, soluble fraction; T, thermolysin-treated chloroplasts.
(A) Import of proteins with known localization used as a control for fraction purity: 16/EGFP (a transit peptide of spinach [*Spinacia oleracea*] OE16 of oxygen evolution system from thylakoid lumen, fused with enhanced GFP) (Marques et al., 2003), LHCP (light-harvesting chlorophyll *a/b* binding pea protein localized in thylakoid membranes) (Tan et al., 2001), and Toc34 (a component of the protein transport complex from the outer envelope membrane) (Chen and Schnell, 1997).
(B) Import of maize PSYs. Arrows, mature processed protein; star, 20-kD band.

maize line B73 used in our experiments, against other PSY sequences available from the National Center for Biotechnology Information database, showed that Thr-257 was characteristic for Zm-PSY1 from 99% of the 79 maize varieties with yellow endosperm. In addition, Thr-257 was found in 30% of the 50 maize lines with white endosperm and two species of teosinte, the wild ancestor of maize that has the ancestral characteristic of white endosperm. Seventy percent of white maize varieties had either Pro-257 or Ser-257; PSYs from all other plants carried Pro at the corresponding position. Asn-168 was found in Zm-PSY1 from all maize varieties, as well as in PSY of teosinte and some grass species; PSYs from other plants carried Ser at the corresponding position (Figure 5).

More detailed analysis of PSY1 sequences from maize and other grasses (Palaisa et al., 2003; Fu et al., 2010) revealed that, indeed, the only difference between Zm-PSY1 amino acid sequences from yellow and white endosperm varieties and teosinte, was Thr/Pro/Ser-257. We also found some sequence differences within the chloroplast transit peptide around positions 52 to 55 (data not shown). Since the transit peptide is processed after chloroplast import and does not affect enzyme activity, we did not include this region in this study.

To test if amino acids in positions 168 and 257 are important for localization, we generated a set of variants from Zm-PSY1 of B73 (for which the allele in yellow endosperm is Asn-168/Thr-257 or NT): with one amino acid change of Asn-168 to Ser (Zm-PSY1-ST) and an independent or additional change of Thr-257 to Pro or Ser (Zm-PSY1-NP, Zm-PSY1-NS, and Zm-PSY1-SP). We also mutated sites, corresponding to 168 and 257, in Zm-PSY2 and Os-PSY1 (see Table 1 for explanation of all PSY variants). PSY variant cDNAs were fused with GFP and expressed in maize protoplasts from both etiolated (Figure 6) and green tissues (data not shown). With the exception of Zm-PSY1-NP, the stromal location of Zm-PSY1 GFP fusions was unchanged. Also, all Zm-PSY2 and Os-PSY1 variants retained localization phenotype to plastoglobuli (data not shown) as seen for the progenitor maize PSY2 or rice PSY1 proteins.

The striking exception was seen in etiolated protoplasts, where Zm-PSY1-NP, naturally found in some white varieties and teosinte, showed a surprising localization phenotype. In plastids of 30% of transformed protoplasts, Zm-PSY1-NP-GFP formed unusual spikes, which stretched chloroplasts from inside, causing a remarkable morphological change of plastid shape, from round elliptical to diamond with sharp corners where spikes touched the envelope membrane (Figure 6; see Supplemental Figure 2 stereogram and Supplemental Movies 1 and 2 online). In the remaining 70% of protoplasts, Zm-PSY1-NP-GFP was localized to stroma, similar to the phenotype exhibited by the

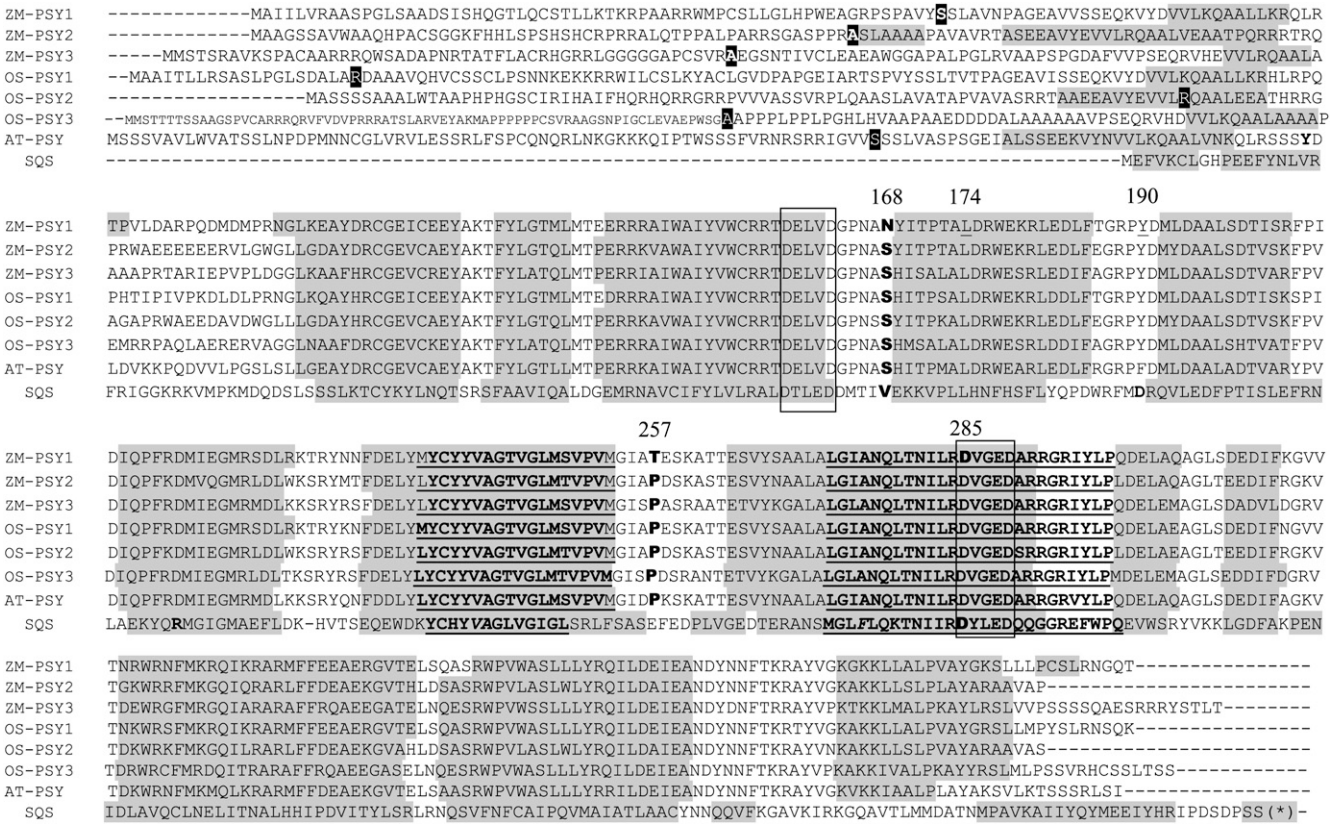

Figure 4. Alignment of PSY Amino Acids for All Enzymes Used in Experiments Adjusted to Secondary SQS Structure.

168, Amino acid represented by Asn (N) in Zm-PSY1 and Ser (S) in all other PSYs; 257, amino acid represented by Thr (T) in Zm-PSY1 and Pro (P) in all other PSYs; 174 and 190, respective amino acids are shown to affect the activity of PSY in cassava (Welsch et al., 2010) and tomato (Gady et al., 2011); 285, mutation at this site inactivates SQS (Gu et al., 1998). Hyphens indicate putative cleavage site for chloroplast transit sequence, predicted by ChloroP. Bold underlining indicates PSY and SQS signature motifs 1 and 2 (conserved pattern). Shading indicates α-helix, predicted by Metaserver based on SQS structure. Box indicates DXXXD putative active site; mutagenesis of Asp-285 inactivates the enzyme. Asterisk indicates that the 62 amino acids of the C terminus of SQS sequence were truncated.

progenitor yellow endosperm Zm-PSY1. That is, a single residue change in the PSY1 protein altered PSY localization and plastid morphology. Remarkably, the double mutation of Zm-PSY1-SP-GFP (where both 168 and 257 sites were mutated) restored stromal localization as exhibited by the progenitor Zm-PSY1. The secondary mutation Asn-168 to Ser-168 appeared to counteract the effect of the single mutation Thr-257 to Pro-257. Interestingly, when Zm-PSY1-NP-GFP was expressed in protoplasts from green seedlings, no fluorescent spikes or drastic morphological change in plastid shape were observed; the phenotype was the same as found with Zm-PSY1 (Figure 1B). The dramatic effect of the single residue change was only apparent in nonphotosynthetic plastids.

To exclude the possible effect of the endogenous Zm-PSY1 on localization of overexpressed Zm-PSY1, we also expressed different PSY-GFP constructs in protoplasts of the *y1-8549* maize line, which lacks PSY1 (Li et al., 2008b), and found no difference in localization of proteins compared with the B73 maize line (see Supplemental Figure 3 online).

The fluorescent spikes observed in Zm-PSY1-NP-GFP expression experiments were similar to fibrils seen in carotenoid-rich chromoplasts of *Solanum capsicastrum* (Wrischer et al., 2007). In *Solanum*, such fibrillar plastoglobuli initiate from globular plastoglobuli. This morphogenic change is observed together with an increase in carotenoid concentration, although it is unknown what triggers fibril formation. Capacity to accumulate large quantities of carotenoids is characteristic of nonphotosynthetic plastids. For example, constitutive overexpression of At-PSY in *Arabidopsis* resulted in carotenoid bar-shaped crystals (spikes) formed in nonphotosynthetic plastids of roots, but no changes were observed in photosynthetic tissues (Maass et al., 2009). Similarly, we did not observe fibrils in green protoplasts, which might be explained by alternative mechanisms of carotenoid sequestration in chloroplasts compared with nonphotosynthetic plastids. Thus, our results suggested that Zm-PSY1-NP was located in fibrillar plastoglobuli, which initiate from globular plastoglobuli in the presence of high concentrations of carotenoids. The presence of carotenoids in fibrils was supported by the use of the Spectral Dye Separation tool in LAS AF software (Leica), applied to the fluorescence intensity spectra of Zm-PSYs-GFP constructs expressed in protoplasts prepared from etiolated leaves of Zm-PSY1 knockout maize (see

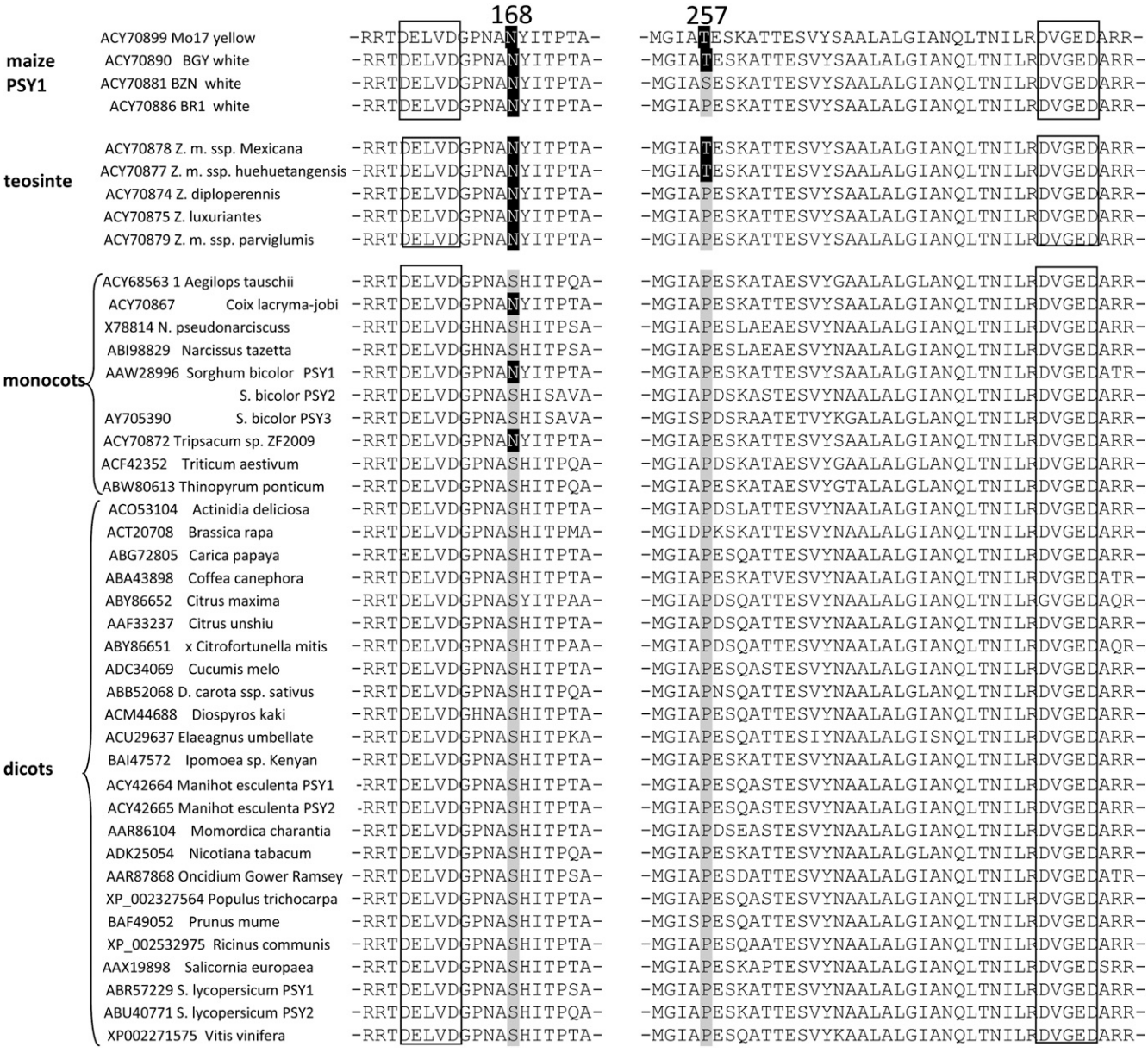

Figure 5. Alignment of PSY Amino Acid Sequences.

BLAST alignment of Zm-PSY1 to all PSY sequences available from the National Center for Biotechnology Information. Box, DXXXD putative active site, based on SQS alignment; highlighting, amino acids 168 and 257. Amino acid numbers refer to Zm-PSY1 sequence.

Supplemental Figure 4 online). The Spectral Dye Separation tool extracted fluorescence of carotenoids from total fluorescence in fibrils (or plastoglobuli, as positive control) of transformed protoplasts, suggesting the presence of carotenoids in those locations.

If fibrils formed as a consequence of high carotenoid production from overexpressed PSY, then inactivation of Zm-PSY1-NP-GFP would be predicted to eliminate fibril formation. To test this hypothesis, we inactivated the enzyme by mutagenesis of the active site. The choice of the active site was based on structural homology of Zm-PSY1 to squalene synthase (SQS), as predicted online by Structure Prediction Meta Server (Ginalski et al., 2003). SQS has a similar catalytic mechanism to PSY and a known crystal structure (Pandit et al., 2000). The PSY active site and other regions critical for enzyme activity are highly conserved among PSY/SQS family members. Meta Server gave a significant 3D-Jury score of 211 (>50 is considered significant) regarding structural similarity between PSY and SQS. Predicted structural similarities between PSYs and SQS are presented in Figure 4. Mutagenesis of either of two highly conserved Asp residues 219 and 223 to Glu inactivates SQS (Gu et al., 1998). Thus, we mutagenized the corresponding Asp residue 285 to Glu and inactivated Zm-PSY1 (Table 1),

Table 1. PSY Variants Used in Transient Expression Experiments

Plant Species	PSY Variant Name	Amino Acid Variation	Is This a Naturally Found Variant?	Test of Activity in *E. coli*	Plastid Localization
Maize	Zm-PSY1	Asn-168; Thr-257	Yes, yellow endosperm lines, including B73, and some white endosperm lines	Active	Stroma/spots
	Zm-PSY1-NP	Asn-168; Pro-257	Yes, white endosperm lines	Active	Fibrils
	Zm-PSY1-NS	Asn-168; Ser-257	Yes, white endosperm lines	–	Stroma
	Zm-PSY1-NP-E	Asn-168; Pro-257; Glu-285	No	Inactive	Stroma
	Zm-PSY1-SP	Ser-168; Pro-257	No	–	Stroma
	Zm-PSY1-ST	Ser-168; Thr-257	No	–	Stroma
	Zm-PSY2	Ser-168; Pro-257	Yes	Active[a]	Plastoglobuli
	Zm-PSY2-ST	Ser-168; Thr-257	No	–	Plastoglobuli
	Zm-PSY2-NP	Asn-168; Pro-257	No	–	Plastoglobuli
	Zm-PSY2-NT	Asn-168; Thr-257	No	–	Plastoglobuli
	Zm-PSY3	Ser-176; Pro-265	Yes	Active[b]	Plastoglobuli
Rice	Os-PSY1	Ser-179; Pro-268	Yes	Active[a]	Plastoglobuli
	Os-PSY1-ST	Ser-179; Thr-268	No	–	Plastoglobuli
	Os-PSY2	Ser-163; Pro-253	Yes	Active[a]	Plastoglobuli
Arabidopsis	At-PSY	Ser-181; Pro-270	Yes	Active[c]	Plastoglobuli

Numbers of amino acids are actual numbers in PSY amino acid sequences. Plastid localization is based on the PSY GFP fusion experiments.
[a]Gallagher et al. (2004).
[b]Li et al. (2008a).
[c]Maass et al. (2009).
–, Was not tested.

which we confirmed by testing for functional complementation in *Escherichia coli* (see Methods). When we expressed the inactive enzyme Zm-PSY1-NP-E-GFP in etiolated protoplasts, the plastid morphology was now normal, fibrils no longer formed, and the inactive enzyme showed a stromal localization as found for the active, progenitor enzyme, Zm-PSY1 (Figure 6). The Spectral Dye separation tool showed no carotenoid fluorescence signal when protoplasts expressed the inactive enzyme Zm-PSY-NP-E compared with the positive signal obtained from protoplasts expressing the active enzyme Zm-PSY-NP (see Supplemental Figure 4 online). Thus, we conclude that increased local carotenoid concentration, causing fibril spikes and plastid morphological change, was due to PSY1 enzyme activity.

Computer Modeling of PSY Structures Provided Insight into Localization Phenotypes of Mutant Enzymes

We hypothesized that changes in the localization phenotype of Zm-PSY1-NP (compared with Zm-PSY1 and Zm-PSY1-NP-E) were related to structural changes in the protein. To study the effect of various residues at positions 168 and 257 on structure of Zm-PSY1, we used the computational methods of structural homology modeling and molecular modeling. Homology modeling provided initial structural predictions for Zm-PSY1 (NT), Zm-PSY1-NP, and Zm-PSY1-SP. Selected structural predictions resulting from our homology modeling calculations were then subjected to minimization and molecular dynamics techniques (see Methods) to derive our final predicted structures. We aligned the latter two structural predictions against that of our predicted structure of Zm-PSY1. The aligned structures of the Thr-257 and Pro-257 variants of Zm-PSY1 (Figure 7A) clearly showed that the overall structure of the enzyme is preserved, in particular the length and relative positions of α-helices, with some perturbations in a few of the loop domains. The overall root mean square deviation (RMSD) between the two structures was 3.8 Å (Figure 7B, red line). Most notable was the large variation in the loop region around residue 184. The loop is located in close proximity to the $_{159}$DELVD$_{163}$ region of the enzyme (Figure 7A), which together with $_{285}$DVGED$_{289}$ is a conserved sequence among isoprenoid synthases and forms an active site to bind phosphate groups of a substrate (Pandit et al., 2000). The deviation between RMSD values of Zm-PSY1 and Zm-PSY1-NP at this region was noted to be significantly larger than 3.8 Å. The difference between Zm-PSY1 and Zm-PSY1-SP (Figure 7B, green line) in the same region, however, was not significant when taking into account the overall average RMSD values difference across the entire protein. This observation suggested that the structure of Zm-PSY1-SP was similar to Zm-PSY1. The similar structure was consistent with the common stromal localization of these two proteins.

Our modeling predicted that a change of Thr to Pro at position 257 will cause remote structural alterations in PSY1 in the loop region around residue 184, where several mutations were shown to affect PSY activity. For example, a change of the amino acid corresponding to Ala-174 to Asp increased PSY activity in cassava (Welsch et al., 2010), but mutagenesis of the amino acid corresponding to Pro-190 to Leu decreased the activity of PSY1 in tomato (*Solanum lycopersicum*; Gady et al., 2011) (all residue numbers are relative to Zm-PSY1 and shown in Figures 4 and 7B in blue). A second amino acid change at Ser-168 ($S_{168}P_{257}$), however, was able to counteract the structural perturbations caused by Pro-257, restoring the structure and specific features

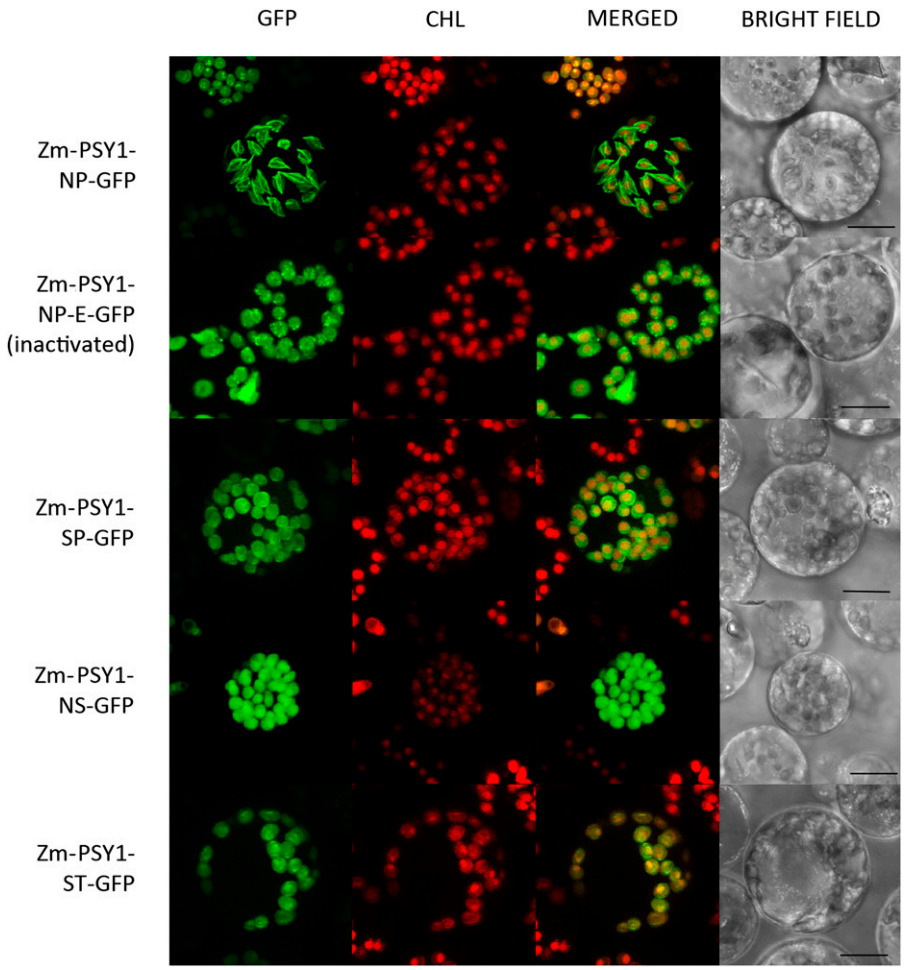

Figure 6. Transient Expression of Zm-PSY1-NP-GFP and Its Mutagenized Variants in Etiolated Maize Protoplasts.

Zm-PSY1-NP forms characteristic spikes in 30% of cases (see central protoplast); the remaining 70% is soluble (top left corner). Zm-PSY1-SP, Zm-PSY1-NS, and Zm-PSY1-ST are localized evenly inside plastids, suggesting soluble stromal localization. CHL, chlorophyll autofluorescence. Bars = 10 μm.

of the progenitor Zm-PSY1. Therefore, PSYs with NT or SP are predicted to be structurally similar, whereas NP is predicted to cause a structural perturbation. Thus, we suggest that a single specific amino acid alteration in PSY1 could change protein folding which could potentially have functional and/or localization consequences. Variation at residue 257, which perturbed the loop region at 184, remote from the catalytic site, affected protein structure and thus altered activity of the enzyme. Such an effect by a distal residue is not unusual, as it is well known that variation of single amino acids at sites distal to the active site, even in flexible loop regions, can affect enzyme catalytic activity through changes in overall protein structure (Peterson and Schachman, 1992; Tomatis et al., 2005; Wang et al., 2006). Structural changes in PSY might also affect pathway flux by alternatively affecting protein–protein interactions with upstream enzyme geranylgeranyl diphosphate synthase, which provides the PSY substrate, or with downstream enzymes (Cuttriss et al., 2011).

DISCUSSION

Cell-Specific Suborganellar Localization of PSY

As a rate-controlling enzyme of the pathway, PSY has been used extensively for metabolic engineering of the carotenoid biosynthetic pathway in plants (Giuliano et al., 2008) despite limited understanding of plastid suborganellar location of the pathway. Confocal microscopy of fluorescently tagged PSYs provided a glimpse into the carotenoid biosynthetic microenvironment in leaf mesophyll cells. For example, the effect of the NP variation on fibril formation occurred in etioplasts from a subpopulation of protoplasts found among the complex population of cell types shown to exist in leaves (Majeran et al., 2010). Whole-tissue carotenoid or proteomic extraction would otherwise have masked these perturbations of enzyme location and carotenoid accumulation taking place in subpopulations of cells. Our approach has elucidated the physical location of a key pathway

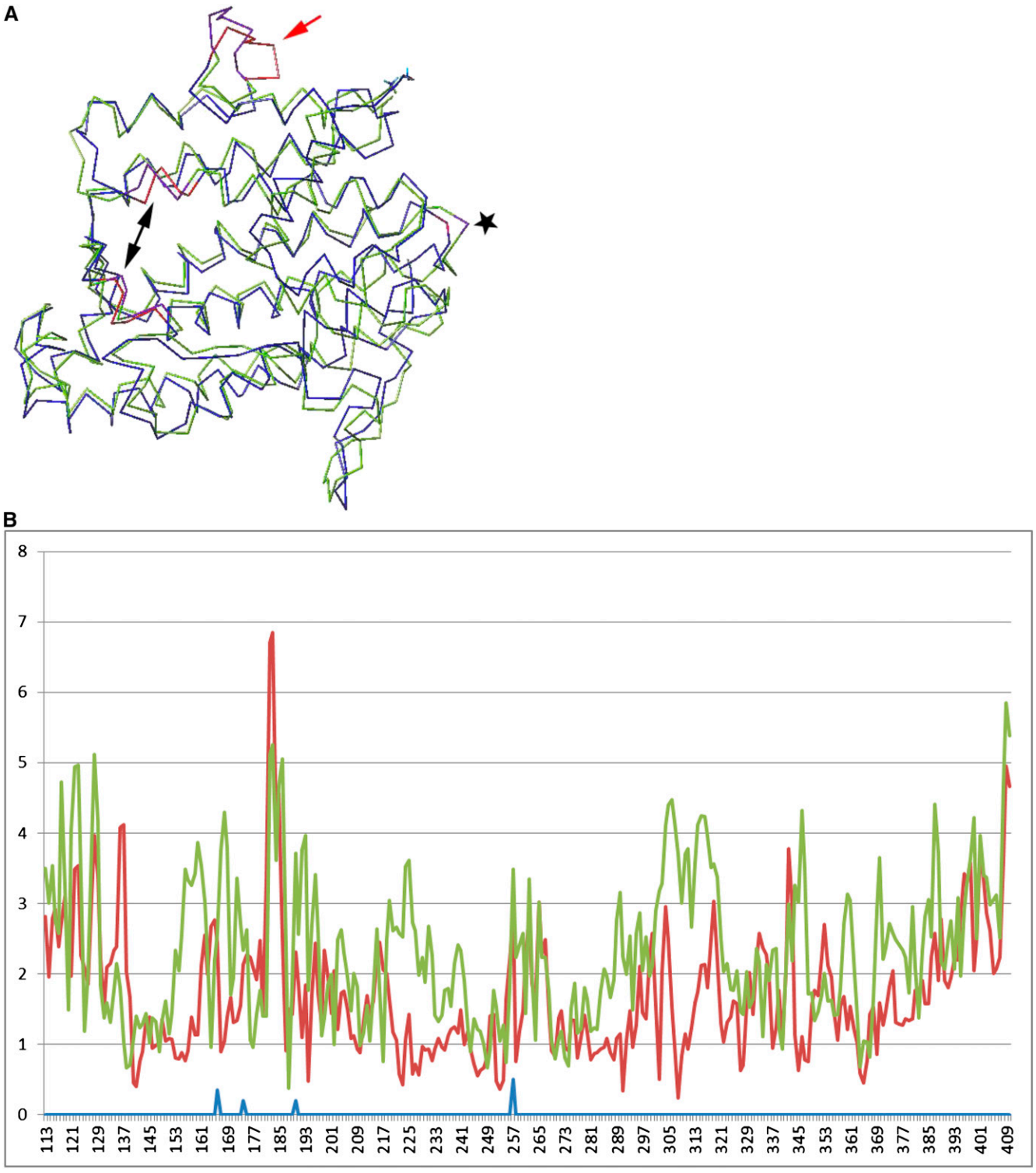

Figure 7. Sequence of Zm-PSY1s with Transit Peptide Removed Threaded onto Crystal Structure of SQS.

(A) Graphical representation of RMSD data on Zm-PSY1 modeling. Blue, Zm-PSY1; green, Zm-PSY1-NP; star, amino acid 257; red arrow, perturbed region; black double arrow, regions $_{159}$DELVD$_{163}$ and $_{285}$DVGED$_{289}$ as putative active sites.

(B) RMSD data showing mean distance (*y* axis, in angstroms) between atoms of the three superimposed Zm-PSY structures (numbered Zm-PSY amino acids shown on the *x* axis). Red, Zm-PSY1-NP; green, Zm-PSY1-SP; blue, marker to show location in sequence of amino acids 168, 174, 190, and 257.

enzyme that must interface with a complex and dynamic metabolon in the context of the suborganellar architecture that is unique to plastid type in specific tissues. More importantly, we discovered that not all PSYs localize identically. This discovery serves as a source of caution and also opportunity for improving carotenoid targets needed, for example, to improve seed nutritional quality or plant stress resistance to address challenges of food security and needs for biofuels in the face of global climate change.

Localization to Plastoglobuli

It is remarkable that PSY isozymes target to unique chloroplast suborganellar sites and that small sequence variation and enzyme activity of PSY1 alters enzyme localization. Plastoglobuli are found in all plastids, although their specific function is not well understood (Bréhélin and Kessler, 2008). Plastoglobuli range in size from 60 to 4000 nm and their composition varies depending on plastid type and plant source (Steinmüller and Tevini, 1985). In chloroplasts, plastoglobuli associate with thylakoids (Austin et al., 2006), while details of plastoglobular association in nonphotosynthetic plastids are sparse. In general, plastoglobuli contain carotenoids, plastoquinones, tocopherols, and various proteins surrounded by a distinctively composed lipid monolayer that is contiguous with the outer layer of the thylakoid lipid bilayer (Kessler et al., 1999; Austin et al., 2006; Ytterberg et al., 2006; Zbierzak et al., 2010). Fibrillins, the major proteins of plastoglobuli (Singh and McNellis, 2011), maintain the structure of the globules and assist in the globular-fibril transition to store high amounts of carotenoids synthesized during chromoplast development (Bréhélin and Kessler, 2008). Plastoglobuli also enlarge and proliferate in response to abiotic stress (e.g., high light, drought, salt, heat, and nitrogen starvation) (Locy et al., 1996; Eymery and Rey, 1999; Bondada and Syvertsen, 2003; Szymańska and Kruk, 2010; Zhang et al., 2010). These stress conditions induce accumulation of carotenoids and/or their apocarotenoid products (Li et al., 2008a, 2008b), and the expression of core plastoglobuli protein genes correlates with the expression of several enzymes from the carotenoid pathway (Lundquist et al., 2012).The importance of plastoglobuli in modulating plant metabolism is beginning to gain attention. Overexpression of the tocopherol cyclase VTE1, a plastoglobular enzyme, resulted in proliferation of plastoglobuli and an increased level of tocopherols (Vidi et al., 2006; Zbierzak et al., 2010). It appears that activity of the overexpressed PSY1, with the naturally occurring NP sequence variation, may exert an effect on fibrillar plastoglobule architecture, since the active enzyme caused plastoglobular fibril formation, which disappeared when the PSY active site was mutated. In both VTE1 and PSY1 cases, overexpression of plastoglobular-associated enzymes caused physical changes in the site of carotenoid sequestration. Taken together, increased levels of rate-controlling plastoglobule-located vitamin E and carotenoid biosynthesis enzymes might drive plastid structural changes needed to provide a sink for the hydrophobic biosynthetic pathway products. Future study of the physical changes associated with PSY-NP overexpression are needed to elucidate the dynamic relationship between expression of active pathway enzyme and morphological transitions at the plastid ultrastructural level.

Open Questions on Metabolon Organization and Dynamics

Establishment of PSY localization leads to the question of how and where the entire pathway is reconstituted. Carotenoids are found on envelope and thylakoid membranes, implying that either the pathway forms on two membrane sites or that carotenoids are transported by an unknown mechanism. Carotenoid metabolons (enzyme complexes) are predicted to exist on the basis of high molecular weight complexes containing PSY or other carotenoid enzymes (Maudinas et al., 1977; Camara et al., 1982; Kreuz et al., 1982; Al-Babili et al., 1996; Bonk et al., 1997; Lopez et al., 2008). A recent study showed that the capacity for enzymes to interact was associated with enhanced carotenoid pathway activity (Quinlan et al., 2012). Metabolon-associated enzymes could facilitate substrate channeling, as has been suggested by the absence of carotenoid pathway intermediates, except in cases where the pathway is artificially blocked (Wurtzel, 2004). But where is the pathway as a whole and how and where are these putative metabolons assembled? *Arabidopsis* PSY localized to plastoglobules (as did maize PSY2 and 3 and rice PSY1, 2, and 3). It is an enigma how PSY is recruited to form a complete pathway. Based on proteomics studies of *Arabidopsis* chloroplasts (Joyard et al., 2009; Ferro et al., 2010), PDS is on the envelope and thylakoid and ζ-carotene desaturase is in the stroma. Together with PSY, it is possible to form a complex to produce prolycopene, a pathway intermediate. The absence of detectable prolycopene suggests that additional enzymes are recruited, but these are not detected by proteomics that may be due to limitations of the proteomics methodologies. In contrast with the enzyme localization seen in *Arabidopsis* chloroplasts, in chromoplasts, which exhibit an exaggerated developmental induction of carotenoid accumulation, the proteomics analysis revealed that most of the enzymes were found in plastoglobules (Ytterberg et al., 2006; Vidi et al., 2007). Therefore, the possibility exists that the complexes are forming in a dynamic fashion and recruited as needed.

Implications for Metabolic Engineering

The findings presented here have significant implications for metabolic engineering of carotenoids in plants, whether the goal is increased nutritional value or to provide enhanced stress resistance in the context of global climate change. Before considering the approach to metabolic engineering of carotenogenesis, it is necessary to consider the temporal scale together with the tissue, cell, and suborganellar specificity where carotenoid biosynthesis is induced in plants. In a given cell carrying a plastid of a given type, carotenoid biosynthesis should be viewed as a dynamic process, where synthesis is induced in response to developmental, biotic, and abiotic signals, both at the short and long term. In a given tissue, this dynamic process is heterogeneous with regard to cell type and function. Thus, when we engineered protoplasts to visualize location of PSY enzymes, we are getting a glimpse into this dynamic process, where in response to certain signals, PSY is locally overexpressed to achieve a desired change in profile of carotenoids destined for specific plastid membranes for a given purpose (e.g., photosynthetic carotenoids on thylakoid membranes or signaling apocarotenoids

derived from the envelope membrane). There are known connections between induction of carotenoid enzymes and physical changes at the subcellular level. For example, morphological changes associated with carotenogenesis in development of chromoplasts include increases in fibrillins, plastoglobules, and biosynthetic enzymes (Deruère et al., 1994). The different suborganellar localizations exhibited by allelic variants suggest that PSYs might be involved in mobilization of carotenoid pathway enzymes to mediate carotenogenesis at distinct locations, may control carotenogenesis by altered localization of PSY, and that localization of an active PSY may influence plastid ultrastructure. Clearly, we show that not all PSYs behave identically, representing an opportunity for metabolic engineering or breeding with specific allelic variants.

Which PSY Variant Is Best for Metabolic Engineering May Depend on Plastid Type and Carotenoid Physiological Role

PSYs are highly conserved in their amino acid sequence (Figure 4). However, we found small variations in a region that must be important for activity because this region lies adjacent to a common signature motif found in isoprenoid synthases (Pandit et al., 2000). It is significant that PSY1 with NT or SP combinations behaved similarly in localization, in contrast with NP, which resulted in fibril formation. The question is then raised whether there is a structural variant that provides optimal function for a particular plastid type.

Both NT and NP types encode functional enzymes. Known PSYs with NP in species of *Tripsacum*, *Coix*, *Sorghum*, and *Zea* do not accumulate endosperm carotenoids due to the lack of *PSY1* endosperm transcription, which is the ancestral state of the PSY1, *y1* locus. Maize *Y1* alleles were selected as dominant alleles that conditioned the yellow carotenogenic endosperm. Examination of PSY1 (*Y1* allele) sequences associated with yellow endosperm revealed that 99% have NT (Palaisa et al., 2003; Fu et al., 2010), which would suggest that NT is the optimal form to mediate endosperm carotenogenesis. The combination of promoter insertion with this unique NT variation may have been ideal for amyloplast carotenogenesis. Indeed, when different PSYs were tested in improvement of endosperm carotenoid levels in Golden Rice (Paine et al., 2005), it was the maize PSY1-NT variant that proved to be most effective compared with PSYs from other species that were tested, although the NP version of maize PSY was not tested. Alternatively, the PSY1-NT variant may have dominated as a consequence of the selective pressure linked to the gain-of-function endosperm expression (Palaisa et al., 2003; Gallagher et al., 2004; Li et al., 2009). Taking into account the ability of the PSY1-NP variant to form concentrated carotenoids and fibrillar structures, the NP variant could be superior to NT for endosperm expression and should be tested.

It is also possible that a stromal localization of Zm-PSY1 might provide an advantage for enzyme performance in amyloplasts without internal membrane structures, while fibril association might play an important role in other plastid types. On the basis of our results of expression in etiolated leaves, it appears that the NP version may offer some advantage as suggested by the formation of fibrillar structures that appear to have carotenoids. Our findings suggest that use of the NP variation may be more effective in enhancing production of carotenoids in certain tissues. For example, PSY1 is naturally expressed in etiolated tissue and known to provide thermal tolerance that is lost in plants that are unable to make PSY1 (Li et al., 2008b). Indeed, if the NP variant is more effective in promoting carotenoids in etioplasts, this allelic variant could be valuable in selecting plants that are more resilient to climate change.

In summary, further studies on the effect of sequence variation are key to metabolic engineering of carotenoids. It will be critical to explore the underlying mechanisms that link specific PSY1 variants with fibril formation and induction of carotenogenesis. Elucidation of how architectural changes affect carotenogenesis will have far-reaching effects on carotenoid metabolic engineering by providing knowledge needed to finely modulate carotenoids destined for specific plastid suborganellar regions. Such a goal is presently unattainable given limitations of our current understanding of the pathway. Our discoveries provide an entry to begin to understand the complexity of how the carotenoid machinery is organized, information that will be critical for metabolic engineering with predictable outcomes. It is apparent that there remain many open questions regarding carotenogenesis and metabolon formation. Further study will shed light on how PSYs contribute to the dynamic assembly and organization of the complex carotenoid metabolons that must form in response to various developmental and stress signals in plastids of various ultrastructure.

METHODS

Plant Material

Pea (*Pisum sativum* var Green Arrow, Jung Seed) was grown in a growth chamber, at 18 to 20°C, 14/10-h dark/light cycle at 425 μmol m^{-2} s^{-1}. Plants were harvested and used for chloroplast isolation after 10 to 14 d. Black-eyed cowpeas (*Vigna unguiculata* subsp *unguiculata*, Vermont Bean Seed) and maize (*Zea mays*) var B73 and *y1-8549* seeds were grown in vermiculite, supplied by water only, for 10 d. B73 was grown both under dark and light conditions and *y1-8549* only in the dark.

Cloning

We used cDNA of the genes from the following sources: *Z. mays* var B73 PSYs, Zm-PSY1, Zm-PSY2 (Gallagher et al., 2004), and Zm-PSY3 (Li et al., 2008a); and *Oryza sativa* var IR36 PSYs Os-PSY1 and Os-PSY2 (Gallagher et al., 2004). pGEM-Os-PSY3 (Welsch et al., 2008) was kindly provided by R. Welsch. *Arabidopsis thaliana* PSY, At-PSY, was ordered as clone DKLAt5G17230 from the ABRC. Maize plastoglobulin 2, Zm-PG2, was ordered as clone ZM_BFc0045D12 from the Arizona Genome Institute. Plasmid pLHCP (from pea) was received as a gift from Kenneth Cline, pBS-OE16/EGFP from J.P. Marques and Ralf B. Klösgen (Martin Luther University Halle-Wittenberg, Germany), and pToc34 (pET21d-IAP34-Nco/NotI-13) from D. Schnell. pFB70 and pFB71 (Breuers et al., 2012) were kindly provided by A. Weber (University of Duesseldorf, Germany).

For chloroplast import experiments, full copies of cDNAs of Zm-PSY1, Zm-PSY2, and Zm-PSY3 were cloned into expression vector pTnT (Promega) according to the manufacturer's instructions, making pTnT-Zm-PSY1, pTnT- Zm-PSY2, and pTnT- Zm-PSY3 vectors, respectively.

For transient expression, cDNAs of Zm-PSY1, Zm-PSY2, Zm-PSY3, Os-PSY1, Os-PSY2, Os-PSY3, and LHCP without stop codons were cloned into pUC35S-sGFP-Nos vector to get a fusion of PSY with GFP under control of cauliflower mosaic virus 35S promoter (pUC35S-sGFP-

Nos vector was constructed based on pUC35S-GUS-Nos and pBIG12 [Okada et al., 2000], which were digested with *Bam*HI/*Eco*RI, and a β-glucuronidase (GUS) cassette from pUC35S-GUS-Nos was replaced with a GFP cassette). The resultant vectors were pUC35S-Zm-PSY1-sGFP-Nos, pUC35S-Zm-PSY2-sGFP-Nos, pUC35S Zm-PSY3-sGFP-Nos, pUC35S-Os-PSY1-sGFP-Nos, pUC35S- Os-PSY2-sGFP-Nos, pUC35S- Os-PSY3-sGFP-Nos, and pUC35S-LHCP-sGFP-Nos. At-PSY and Zm-PG2 were cloned into pSAT6(A)-RFP-N1 vector (Citovsky et al., 2008) to get a fusion with RFP. The resultant vectors were pSAT-At-PSY-RFP and pSAT-Zm-PG2-RFP.

Site-directed mutagenesis of amino acids 168 and 257 in PSY1 and corresponding residues in other PYSs was performed with QuikChange Lightning site-directed mutagenesis kit (Agilent Technologies) according to the manufacturer's instructions.

For *Escherichia coli* complementation, pBS-Zm-PSY1 (Gallagher et al., 2004) was site-directly mutagenized as described above, resulting in pBS-Zm-PSY1-NP and pBS-Zm-PSY1-D_{285}E (inactivated).

All cloning was confirmed by sequencing at MWG Operon Sequence Facility. For details on cloning, see Supplemental Table 1 online.

Preparation of Precursors for Chloroplast Import

Genes were transcribed and translated in vitro with SP6 polymerase in rabbit reticulocyte lysate by a TnT-coupled system (Promega) in the presence of 35S-metionine (Perkin-Elmer).

Chloroplast Isolation and Protein Import

To prevent starch accumulation, plant leaves were collected after 8 h of dark and then ground with a kitchen blender in grinding buffer (50 mM HEPES, pH 8, 330 mM sorbitol, 1 mM $MnCl_2$, 1 mM $MgCl_2$, 2 mM EDTA, 0.2% [w/v] BSA, and 0.1% [w/v] ascorbic acid), at 4°C, and filtered through two layers of cheesecloth and 60-μm nylon filter. Chloroplasts were isolated from the resultant suspension using Percoll gradient centrifugation (Bruce et al., 1994). Percoll gradients were prepared by centrifugation of 50% Percoll (Sigma-Aldrich) in the grinding buffer (40,000*g*, 30 min, 4°C). The chloroplast suspension was layered on the top of the gradient and centrifuged at 12,000*g*, at 4°C, for 10 min. The lower band, containing intact chloroplasts, was aspirated, collected, and washed with the cold import buffer (50 mM HEPES, pH 8, and 330 mM sorbitol), 800*g*, 4°C, for 2 min. Intact chloroplasts were resuspended in 140 μL/reaction of cold import mix (50 mM HEPES, pH 8, 330 mM sorbitol, 4 mM Met, 4 mM ATP, 4 mM $MgCl_2$, 10 mM K-Ac, and 10 mM $NaHCO_3$) at a concentration of 50 μg of chlorophyll/reaction. For the import reaction, 10 μL of in vitro transcription/translation product was added to the chloroplast mix. After 25 min (25°C, light), the import reaction was stopped by placing on ice and diluting with 500 μL of cold import buffer, chloroplasts were collected by centrifugation (800*g*, 2 min), diluted in 200 μL of fresh cold import buffer supplemented with 1 mM $CaCl_2$, and divided into two parts: one was left intact, the other was treated with 125 ng/μL of thermolysin (30 min on ice). The reaction was stopped by adding EDTA to a final concentration of 10 mM. Chloroplasts were collected by centrifugation (800*g*, 2 min). Sample buffer for SDS-PAGE was added to the pellets and the protein extracts were analyzed by gel electrophoresis.

For fractionation experiments after the import reaction, intact chloroplasts were washed twice with import buffer, then diluted with HL buffer (10 mM HEPES-KOH and 10 mM $MgCl_2$, pH 8), and total mixture was frozen in liquid nitrogen/thawed three times, than centrifuged (16,000*g*, 20 min). Supernatant, containing soluble chloroplast proteins, and the pellet, containing membrane fraction, were analyzed by SDS-PAGE gel. Alkaline treatment of membrane fractions was performed with 200 mM Na_2CO_3, pH >10, 10 min on ice, and then the pellet containing treated membranes was separated from the supernatant by centrifugation (16,000*g*, 20 min) and analyzed by SDS-PAGE. A signal from radiolabeled protein was analyzed by the Storm PhosphorImager (Molecular Dynamics).

Protoplast Isolation and Transient Expression

Cowpea mesophyll protoplasts were isolated from cotyledon leaves and transfected with vectors containing GFP fusion proteins, by polyethylene glycol–mediated transformation (van Bokhoven et al., 1993). The epidermal cell layer from 10-d-old cotyledon leaves was peeled off the lower side of the leaves and treated in a Petri dish with an enzyme solution (0.5% cellulase [from *Trichoderma viridae*; Sigma-Aldrich], 0.05% pectinase [from *Rhizopus* sp; Sigma-Aldrich], 0.6 M mannitol, 10 mM $CaCl_2$, and 20 mM MES, pH 5.6) for 3.5 h with gentle agitation, followed by 5 min of vigorous shaking. Released protoplasts were collected through the 60-μm nylon filter and washed three times with Ca/mannitol solution (0.6 M mannitol, 10 mM $CaCl_2$, and 20 mM MES, pH 5.6), 80*g*, 4°C, for 5 min. A purified plasmid vector DNA (10 μg in 10 μL ice-cold Tris, pH 8.5) was added to 10^6 protoplasts in 150 μL 0.6 M mannitol containing 10 mM $CaCl_2$ and immediately diluted with 500 μL solution of polyethylene glycol solution [40% polyethylene glycol 6000, 0.5 M mannitol, and 0.1 M Ca $(NO_3)_2$]. The protoplast suspension was gently mixed for 10 to 15 s, diluted with 4.5 mL mannitol/MES solution (0.5 M mannitol, 15 mM $MgCl_2$, and 0.1% MES pH 5.6), and kept at room temperature for 20 min. The protoplasts were then washed with 0.6 M mannitol and 10 mM $CaCl_2$ and incubated for 12 to 16 h at 25°C on a table.

Maize leaf protoplasts were isolated according to Sheen (2002; http://genetics.mgh.harvard.edu/sheenlab/protocols_reg.html) from the middle part of the second leaf of either dark- or light-grown plants. Leaves were collected from 20 plants and chopped perpendicularly into 1-mm pieces with a razor blade. Chopped tissue was vacuum infiltrated with enzyme solution (1.5% cellulase [Onozuka R10 from *T. viridae*; Sigma-Aldrich], 0.3% pectinase [from *Rhizopus* sp; Sigma-Aldrich], 0.1% BSA, 5 mM β-mercaptoethanol, 0.6 M mannitol, 10 mM $CaCl_2$, and 20 mM MES, pH 5.7) and incubated under gentle shaking for 2 h. Released protoplasts were collected, washed, and subjected to polyethylene glycol–induced transformation as described above.

Each transient expression experiment was repeated seven to 10 times. Transformation efficiency was 60 to 80%.

Confocal Microscopy

Transient expression of GFP and RFP fusion proteins was visualized with a DMI6000B inverted confocal microscope with TCS SP5 system (Leica Microsystems CMS). Five to seven microscope fields under magnification ×20, ~1000 cells each, were examined for every transient expression experiment.

Oil or water immersion objective (×63) was used in all cases. A 488-nm argon laser was used to excite the fluorescence of enhanced GFP and chlorophyll, and a 543-nm laser was used to excite RFP. The chloroplast autofluorescence was detected between 664 and 696 nm, and the enhanced GFP fluorescence was detected between 500 and 539 nm and always confirmed by recording the emission spectrum by wavelength scanning (λ-scan) between 500 and 600 nm with a 3-nm detection window. The RFP fluorescence was detected between 600 and 650 nm and emission spectrum confirmed by scanning between 570 and 700 nm. LAS AF software (Leica Microsystems CMS) was used for image acquisition. Images were obtained by combining several confocal Z-planes and subjected to deconvolution. Representative images were used for figures.

Spectral Dye Separation

Separation of spectra of GFP and carotenoids was made using LAS AF software (Leica Microsystems). Carotenoids have a low fluorescence

emission between 500 and 650 nm that can be excited by a 488-nm laser (Vermaas et al., 2008). The software separates the carotenoid emission from the GFP emission. To eliminate any background carotenoid fluorescence in the absence of a PSY transgene, we used protoplasts prepared from Zm-PSY1 knockout maize *y1-8549*, which are unable to produce carotenoids in the absence of the transgenically supplied PSY (Li et al., 2008b). Emission intensity spectra (λ-scans) of soluble cytoplasmic GFP and of β-carotene (see Supplemental Figure 4 online), excited by 488-nm argon laser and collected between 500 and 650 nm for both cases, were used as references. The λ-scan of the image of interest was performed using the same settings, and the emission intensity spectrum was separated into two using references of GFP and carotenoid spectra by Spectral Dye Separation tool, resulting in maximum projection of the λ-scan for each fluorophore.

Soluble cytoplasmic GFP, used as a negative control and GFP spectrum reference, showed no carotenoid emission (see Supplemental Figure 4A online). Fibrils formed by Zm-PSY1-NP (see Supplemental Figure 4B online) have bright fluorescence in the carotenoid channel, suggesting presence of concentrated carotenoids. Such fluorescence disappeared, showing no fibrils when nonactive Zm-PSY1-NP-E was overexpressed in etioplasts (see Supplemental Figure 4C online). A low level of carotenoid fluorescence was observed in etioplasts carrying overexpressed Zm-PSY1-NT (see Supplemental Figure 4D online), which might be due to a basal level of carotenoid biosynthesis in leaves due to inactivity of $_{zm}$PSY when not attached to membranes (Schledz et al., 1996). Punctuated dots, formed in etioplasts by Zm-PSY2-GFP and Zm-PSY3-GFP (see Supplemental Figures 4E and 4F online), also show bright fluorescence in the carotenoid channel, suggesting presence of concentrated carotenoids. By contrast, background level of fluorescence is observed when a noncarotenoid protein is introduced, light-harvesting chlorophyll protein (see Supplemental Figure 4G online).

Functional Complementation Test for Enzyme Activity in *E. coli*

Loss of activity was confirmed by functional complementation of *E. coli* TOP10 carrying pACCAR25ΔcrtB (Gallagher et al., 2004). PSYs were expressed in an *E. coli* strain carrying a pathway of carotenoid genes necessary for making zeaxanthin diglucoside but lacking PSY. In this system, Zm-PSY1 and Zm-PSY1-NP complemented the pathway lesion as seen by the restored production of zeaxanthin diglucoside; Zm-PSY1-D_{285}E transformants were unable to produce zeaxanthin diglucoside, indicating that the mutation inactivated the enzyme (see Supplemental Figure 5 online).

Structural Modeling of Zm-PSY1

The prediction of protein structures was performed by threading the sequence of Zm-PSY1 (B73 type) without chloroplast transit sequence onto the SQS template (1EZF) using MODELER (Šali et al., 1995) and Rosetta (Leaver-Fay et al., 2011) software. The threaded structure was initially subjected to molecular modeling energy minimization techniques using SYBYL-X 1.2 (Tripos International) to reduce steric strain present in the threaded structure. The minimized structure was then entered into molecular dynamics (MD) simulation from which an average structure of Zm-PSY1 from a 500-ps trajectory was determined. From the modeled average structure, structures for the polymorphic forms Zm-PSY1-NP, Zm-PSY1-SP, and Zm-PSY1-NS were determined using molecular modeling only. Using SYBYL, we computationally mutated the residue at the 257 and/or 168 positions by editing the atoms in the model and applied the same procedure of energy minimization and molecular dynamics, which resulted in average structures for these polymorphic forms of the enzyme. Alignment of the corresponding C-alpha carbons of each residue in these structures to original Zm-PSY1 was made using the Homology Modeling and Alignment tool in SYBYL.

Accession Numbers

Sequence data from this article can be found in the Arabidopsis Genome Initiative or GenBank/EMBL databases under the following accession numbers: for maize: PSY1, AAR08445; PSY2, AAX13807; PSY3, DQ356430; PG2, BT039786_1; for rice: PSY1, AY445521; PSY2, AY773943; PSY3, FJ214953; for *Arabidopsis*: PSY, AT5G17230; and for pea: Toc34, L36856.1.

Supplemental Data

The following materials are available in the online version of this article.

Supplemental Figure 1. Overexpression of Proteins with Known Location in Etiolated Maize Protoplasts.

Supplemental Figure 2. Hidden 3D (Third Eye) Stereogram of Transiently Expressed Zm-PSY1-NP-GFP in Etiolated Maize Protoplasts.

Supplemental Figure 3. Transient Expression of Zm-PSY-GFP Variants in Etiolated Maize Protoplasts from PSY1 Knockout Line.

Supplemental Figure 4. Spectral Dye Separation for Transiently Expressed GFP Fusion Proteins in Maize PSY1 Knockout Leaf Protoplasts.

Supplemental Figure 5. *E. coli* Complementation Test.

Supplemental Table 1. Plasmids and Primers Used for Cloning.

Supplemental Movie 1. Zm-PSY1-NT-GFP Localization.

Supplemental Movie 2. Zm-PSY1-NP-GFP Localization.

ACKNOWLEDGMENTS

We thank Kenneth Cline for providing plasmid pLHCP, João P. Marques and Ralf B. Klösgen for providing pBS-16/EGFP, Danny Schnell for providing pToc34, Vitaly Citovsky for pSAT6(A)-RFP-N1, Andreas Weber and Frederique Breuers for plasmids pFB70 and pFB71, and Ralf Welsch for plasmid $_{os}$PSY3-GFP. We thank Changfu Zhu and Yao Xiaoling for technical help and Yaakov Tadmor for helpful discussions. Funding from the National Institutes of Health (GM081160 to E.T.W.) is gratefully acknowledged.

AUTHOR CONTRIBUTIONS

M.S. designed the research and performed the experiments. L.M.T.B. participated in experimental design and performance. R.R.M. designed and analyzed the computational experiments. E.T.W. designed and guided the research. All authors contributed to the analysis of the results and preparation of the article.

Received August 16, 2012; revised August 16, 2012; accepted September 5, 2012; published September 28, 2012.

REFERENCES

Al-Babili, S., von Lintig, J., Haubruck, H., and Beyer, P. (1996). A novel, soluble form of phytoene desaturase from *Narcissus pseudonarcissus* chromoplasts is Hsp70-complexed and competent for flavinylation, membrane association and enzymatic activation. Plant J. **9:** 601–612.

Arango, J., Wüst, F., Beyer, P., and Welsch, R. (2010). Characterization of phytoene synthases from cassava and their involvement in abiotic stress-mediated responses. Planta **232:** 1251–1262.

Auldridge, M.E., Block, A., Vogel, J.T., Dabney-Smith, C., Mila, I., Bouzayen, M., Magallanes-Lundback, M., DellaPenna, D., McCarty, D.R., and Klee, H.J. (2006). Characterization of three members of the *Arabidopsis* carotenoid cleavage dioxygenase family demonstrates the divergent roles of this multifunctional enzyme family. Plant J. **45:** 982–993.

Austin, J.R., IIFrost, E., Vidi, P.-A., Kessler, F., and Staehelin, L.A. (2006). Plastoglobules are lipoprotein subcompartments of the chloroplast that are permanently coupled to thylakoid membranes and contain biosynthetic enzymes. Plant Cell **18:** 1693–1703.

Bondada, B.R., and Syvertsen, J.P. (2003). Leaf chlorophyll, net gas exchange and chloroplast ultrastructure in citrus leaves of different nitrogen status. Tree Physiol. **23:** 553–559.

Bonk, M., Hoffmann, B., Von Lintig, J., Schledz, M., Al-Babili, S., Hobeika, E., Kleinig, H., and Beyer, P. (1997). Chloroplast import of four carotenoid biosynthetic enzymes *in vitro* reveals differential fates prior to membrane binding and oligomeric assembly. Eur. J. Biochem. **247:** 942–950.

Bréhélin, C., and Kessler, F. (2008). The plastoglobule: A bag full of lipid biochemistry tricks. Photochem. Photobiol. **84:** 1388–1394.

Breuers FKH, Braeutigam A, Geimer S, Welzel UY, Stefano G, Renna L, Brandizzi F, Weber APM (2012). Dynamic remodeling of the plastid envelope membranes - A tool for chloroplast envelope *in vivo* localizations. Front. Plant Sci. **3: 7**.

Bruce, B.D., Perry, S., Froehlich, J., and Keegstra, K. (1994). In vitro import of protein into chloroplasts. In Plant Molecular Biology Manual, Vol. J1, S.B. Gelvin and R.B. Schilperoort, eds (Boston: Kluwer Academic Publishers), pp. 1–15.

Camara, B., Bardat, F., and Monéger, R. (1982). Sites of biosynthesis of carotenoids in *Capsicum* chromoplasts. Eur. J. Biochem. **127:** 255–258.

Chen, D., and Schnell, D.J. (1997). Insertion of the 34-kDa chloroplast protein import component, IAP34, into the chloroplast outer membrane is dependent on its intrinsic GTP-binding capacity. J. Biol. Chem. **272:** 6614–6620.

Citovsky, V., Gafni, Y., and Tzfira, T. (2008). Localizing protein-protein interactions by bimolecular fluorescence complementation in planta. Methods **45:** 196–206.

Crawford, A.C., Stefanova, K., Lambe, W., McLean, R., Wilson, R., Barclay, I., and Francki, M.G. (2011). Functional relationships of phytoene synthase 1 alleles on chromosome 7A controlling flour colour variation in selected Australian wheat genotypes. Theor. Appl. Genet. **123:** 95–108.

Cuttriss, A.J., Cazzonelli, C.I., Wurtzel, E.T., and Pogson, B.J. (2011). Carotenoids. In Biosynthesis of Vitamins in Plants, Vol. 58, F. Rébeillé and R. Douce, eds (Amsterdam, The Netherlands: Elsevier), pp. 1–36.

Dall'Osto, L., Fiore, A., Cazzaniga, S., Giuliano, G., and Bassi, R. (2007). Different roles of α- and β-branch xanthophylls in photosystem assembly and photoprotection. J. Biol. Chem. **282:** 35056–35068.

Davison, P.A., Hunter, C.N., and Horton, P. (2002). Overexpression of beta-carotene hydroxylase enhances stress tolerance in *Arabidopsis*. Nature **418:** 203–206.

Denecke, J., Aniento, F., Frigerio, L., Hawes, C., Hwang, I., Mathur, J., Neuhaus, J.-M., and Robinson, D.G. (2012). Secretory pathway research: The more experimental systems the better. Plant Cell **24:** 1316–1326.

Deruère, J., Römer, S., d'Harlingue, A., Backhaus, R.A., Kuntz, M., and Camara, B. (1994). Fibril assembly and carotenoid overaccumulation in chromoplasts: A model for supramolecular lipoprotein structures. Plant Cell **6:** 119–133.

Egea, I., Barsan, C., Bian, W., Purgatto, E., Latché, A., Chervin, C., Bouzayen, M., and Pech, J.C. (2010). Chromoplast differentiation: current status and perspectives. Plant Cell Physiol. **51:** 1601–1611.

Eymery, F., and Rey, P. (1999). Immunocytolocalization of CDSP 32 and CDSP 34, two chloroplastic drought-induced stress proteins in *Solanum tuberosum* plants. Plant Physiol. Biochem. **37:** 305–312.

Faraco, M., Di Sansebastiano, G.P., Spelt, K., Koes, R.E., and Quattrocchio, F.M. (2011). One protoplast is not the other! Plant Physiol. **156:** 474–478.

Fernandez, M.G.S., Hamblin, M.T., Li, L., Rooney, W.L., Tuinstra, M.R., and Kresovich, S. (2008). Quantitative trait loci analysis of endosperm color and carotenoid content in sorghum grain. Crop Sci. **48:** 1732–1743.

Ferro, M., et al. (2010). AT_CHLORO, a comprehensive chloroplast proteome database with subplastidial localization and curated information on envelope proteins. Mol. Cell. Proteomics **9:** 1063–1084.

Friso, G., Majeran, W., Huang, M., Sun, Q., and van Wijk, K.J. (2010). Reconstruction of metabolic pathways, protein expression, and homeostasis machineries across maize bundle sheath and mesophyll chloroplasts: Large-scale quantitative proteomics using the first maize genome assembly. Plant Physiol. **152:** 1219–1250.

Fu, Z., Yan, J., Zheng, Y., Warburton, M.L., Crouch, J.H., and Li, J.-S. (2010). Nucleotide diversity and molecular evolution of the *PSY1* gene in *Zea mays* compared to some other grass species. Theor. Appl. Genet. **120:** 709–720.

Gady, A., Vriezen, W., Van de Wal, M., Huang, P., Bovy, A., Visser, R., and Bachem, C. (2011). Induced point mutations in the phytoene synthase 1 gene cause differences in carotenoid content during tomato fruit ripening. Mol. Breed. **29:** 801–812.

Gallagher, C.E., Matthews, P.D., Li, F., and Wurtzel, E.T. (2004). Gene duplication in the carotenoid biosynthetic pathway preceded evolution of the grasses. Plant Physiol. **135:** 1776–1783.

Ginalski, K., Elofsson, A., Fischer, D., and Rychlewski, L. (2003). 3D-Jury: A simple approach to improve protein structure predictions. Bioinformatics **19:** 1015–1018.

Giorio, G., Stigliani, A.L., and D'Ambrosio, C. (2008). Phytoene synthase genes in tomato (*Solanumlycopersicum* L.) - New data on the structures, the deduced amino acid sequences and the expression patterns. FEBS J. **275:** 527–535.

Giuliano, G., Tavazza, R., Diretto, G., Beyer, P., and Taylor, M.A. (2008). Metabolic engineering of carotenoid biosynthesis in plants. Trends Biotechnol. **26:** 139–145.

Gu, P., Ishii, Y., Spencer, T.A., and Shechter, I. (1998). Function-structure studies and identification of three enzyme domains involved in the catalytic activity in rat hepatic squalene synthase. J. Biol. Chem. **273:** 12515–12525.

Harjes, C.E., Rocheford, T.R., Bai, L., Brutnell, T.P., Kandianis, C.B., Sowinski, S.G., Stapleton, A.E., Vallabhaneni, R., Williams, M., Wurtzel, E.T., Yan, J., and Buckler, E.S. (2008). Natural genetic variation in *lycopene epsilon cyclase* tapped for maize biofortification. Science **319:** 330–333.

Havaux, M., Dall'osto, L., and Bassi, R. (2007). Zeaxanthin has enhanced antioxidant capacity with respect to all other xanthophylls in Arabidopsis leaves and functions independent of binding to PSII antennae. Plant Physiol. **145:** 1506–1520.

Iniesta, A.A., Cervantes, M., and Murillo, F.J. (2008). Conversion of the lycopene monocyclase of *Myxococcus xanthus* into a bicyclase. Appl. Microbiol. Biotechnol. **79:** 793–802.

Jeffrey, S.W., Douce, R., and Benson, A.A. (1974). Carotenoid transformations in the chloroplast envelope. Proc. Natl. Acad. Sci. USA **71:** 807–810.

Johnson, M.P., Havaux, M., Triantaphylidès, C., Ksas, B., Pascal, A.A., Robert, B., Davison, P.A., Ruban, A.V., and Horton, P. (2007).

Elevated zeaxanthin bound to oligomeric LHCII enhances the resistance of Arabidopsis to photooxidative stress by a lipid-protective, antioxidant mechanism. J. Biol. Chem. **282:** 22605–22618.

Joyard, J., Ferro, M., Masselon, C., Seigneurin-Berny, D., Salvi, D., Garin, J., and Rolland, N. (2009). Chloroplast proteomics and the compartmentation of plastidial isoprenoid biosynthetic pathways. Mol. Plant **2:** 1154–1180.

Kessler, F., Schnell, D., and Blobel, G. (1999). Identification of proteins associated with plastoglobules isolated from pea (*Pisum sativum* L.) chloroplasts. Planta **208:** 107–113.

Kreuz, K., Beyer, P., and Kleinig, H. (1982). The site of carotenogenic enzymes in chromoplasts from *Narcissus pseudonarcissus* L. Planta **154:** 66–69.

Leaver-Fay, A., et al. (2011). ROSETTA3: An object-oriented software suite for the simulation and design of macromolecules. Methods Enzymol. **487:** 545–574.

Li, F., Tsfadia, O., and Wurtzel, E.T. (2009). The *phytoene synthase* gene family in the Grasses: subfunctionalization provides tissue-specific control of carotenogenesis. Plant Signal. Behav. **4:** 208–211.

Li, F., Vallabhaneni, R., and Wurtzel, E.T. (2008a). *PSY3*, a new member of the phytoene synthase gene family conserved in the Poaceae and regulator of abiotic stress-induced root carotenogenesis. Plant Physiol. **146:** 1333–1345.

Li, F., Vallabhaneni, R., Yu, J., Rocheford, T., and Wurtzel, E.T. (2008b). The maize phytoene synthase gene family: Overlapping roles for carotenogenesis in endosperm, photomorphogenesis, and thermal stress tolerance. Plant Physiol. **147:** 1334–1346.

Locy, R.D., Chang, C.C., Nielsen, B.L., and Singh, N.K. (1996). Photosynthesis in salt-adapted heterotrophic tobacco cells and regenerated plants. Plant Physiol. **110:** 321–328.

Lopez, A.B., Yang, Y., Thannhauser, T.W., and Li, L. (2008). Phytoene desaturase is present in a large protein complex in the plastid membrane. Physiol. Plant. **133:** 190–198.

Lundquist, P.K., Poliakov, A., Bhuiyan, N.H., Zybailov, B., Sun, Q., and van Wijk, K.J. (2012). The functional network of the Arabidopsis plastoglobule proteome based on quantitative proteomics and genome-wide coexpression analysis. Plant Physiol. **158:** 1172–1192.

Maass, D., Arango, J., Wüst, F., Beyer, P., and Welsch, R. (2009). Carotenoid crystal formation in *Arabidopsis* and carrot roots caused by increased phytoene synthase protein levels. PLoS ONE **4:** e6373.

Majeran, W., Friso, G., Ponnala, L., Connolly, B., Huang, M., Reidel, E., Zhang, C., Asakura, Y., Bhuiyan, N.H., Sun, Q., Turgeon, R., and van Wijk, K.J. (2010). Structural and metabolic transitions of C4 leaf development and differentiation defined by microscopy and quantitative proteomics in maize. Plant Cell **22:** 3509–3542.

Marques, J.P., Dudeck, I., and Klösgen, R.B. (2003). Targeting of EGFP chimeras within chloroplasts. Mol. Genet. Genomics **269:** 381–387.

Maudinas, B., Bucholtz, M.L., Papastephanou, C., Katiyar, S.S., Briedis, A.V., and Porter, J.W. (1977). The partial purification and properties of a phytoene synthesizing enzyme system. Arch. Biochem. Biophys. **180:** 354–362.

Messing, S.A., Gabelli, S.B., Echeverria, I., Vogel, J.T., Guan, J.C., Tan, B.C., Klee, H.J., McCarty, D.R., and Amzel, L.M. (2010). Structural insights into maize viviparous14, a key enzyme in the biosynthesis of the phytohormone abscisic acid. Plant Cell **22:** 2970–2980.

Moran, N.A., and Jarvik, T. (2010). Lateral transfer of genes from fungi underlies carotenoid production in aphids. Science **328:** 624–627.

Okada, K., Saito, T., Nakagawa, T., Kawamukai, M., and Kamiya, Y. (2000). Five geranylgeranyl diphosphate synthases expressed in different organs are localized into three subcellular compartments in *Arabidopsis*. Plant Physiol. **122:** 1045–1056.

Paine, J.A., Shipton, C.A., Chaggar, S., Howells, R.M., Kennedy, M.J., Vernon, G., Wright, S.Y., Hinchliffe, E., Adams, J.L., Silverstone, A.L., and Drake, R. (2005). Improving the nutritional value of Golden Rice through increased pro-vitamin A content. Nat. Biotechnol. **23:** 482–487.

Palaisa, K.A., Morgante, M., Williams, M., and Rafalski, A. (2003). Contrasting effects of selection on sequence diversity and linkage disequilibrium at two phytoene synthase loci. Plant Cell **15:** 1795–1806.

Pandit, J., Danley, D.E., Schulte, G.K., Mazzalupo, S., Pauly, T.A., Hayward, C.M., Hamanaka, E.S., Thompson, J.F., and Harwood, H.J. Jr. (2000). Crystal structure of human squalene synthase. A key enzyme in cholesterol biosynthesis. J. Biol. Chem. **275:** 30610–30617.

Peterson, C.B., and Schachman, H.K. (1992). Long range effects of amino acid substitutions in the catalytic chain of aspartate transcarbamoylase. Localized replacements in the carboxyl-terminal alpha-helix cause marked alterations in allosteric properties and intersubunit interactions. J. Biol. Chem. **267:** 2443–2450.

Pozniak, C.J., Knox, R.E., Clarke, F.R., and Clarke, J.M. (2007). Identification of QTL and association of a phytoene synthase gene with endosperm colour in durum wheat. Theor. Appl. Genet. **114:** 525–537.

Qin, X., Coku, A., Inoue, K., and Tian, L. (2011). Expression, subcellular localization, and cis-regulatory structure of duplicated phytoene synthase genes in melon (*Cucumis melo* L.). Planta **234:** 737–748.

Quinlan, R.F., Shumskaya, M., Bradbury, L.M., Beltrán, J., Ma, C., Kennelly, E.J., and Wurtzel, E.T. (2012). Synergistic interactions between carotene ring hydroxylases drive lutein formation in plant carotenoid biosynthesis. Plant Physiol. **160:** 204–214.

Rodríguez-Suárez, C., Atienza, S.G., and Pistón, F. (2011). Allelic variation, alternative splicing and expression analysis of *Psy1* gene in *Hordeum chilense* Roem. et Schult. PLoS ONE **6:** e19885.

Šali, A., Potterton, L., Yuan, F., van Vlijmen, H., and Karplus, M. (1995). Evaluation of comparative protein modeling by MODELLER. Proteins **23:** 318–326.

Schledz, M., al-Babili, S., von Lintig, J., Haubruck, H., Rabbani, S., Kleinig, H., and Beyer, P. (1996). Phytoene synthase from *Narcissus pseudonarcissus*: Functional expression, galactolipid requirement, topological distribution in chromoplasts and induction during flowering. Plant J. **10:** 781–792.

Siefermann-Harms, D. (1978). Light-induced changes of the carotenoid levels in chloroplast envelopes. Plant Physiol. **61:** 530–533.

Singh, D.K., and McNellis, T.W. (2011). Fibrillin protein function: The tip of the iceberg? Trends Plant Sci. **16:** 432–441.

Steinmüller, D., and Tevini, M. (1985). Composition and function of plastoglobuli. Planta **163:** 201–207.

Szymańska, R., and Kruk, J. (2010). Plastoquinol is the main prenyllipid synthesized during acclimation to high light conditions in Arabidopsis and is converted to plastochromanol by tocopherol cyclase. Plant Cell Physiol. **51:** 537–545.

Tan, B.C., Cline, K., and McCarty, D.R. (2001). Localization and targeting of the VP14 epoxy-carotenoid dioxygenase to chloroplast membranes. Plant J. **27:** 373–382.

Tomatis, P.E., Rasia, R.M., Segovia, L., and Vila, A.J. (2005). Mimicking natural evolution in metallo-β-lactamases through second-shell ligand mutations. Proc. Natl. Acad. Sci. USA **102:** 13761–13766.

Tomato Genome Consortium (2012). The tomato genome sequence provides insights into fleshy fruit evolution. Nature **485:** 635–641.

Vallabhaneni, R., Gallagher, C.E., Licciardello, N., Cuttriss, A.J., Quinlan, R.F., and Wurtzel, E.T. (2009). Metabolite sorting of

a germplasm collection reveals the *hydroxylase3* locus as a new target for maize provitamin A biofortification. Plant Physiol. **151:** 1635–1645.

Vallabhaneni, R., and Wurtzel, E.T. (2009). Timing and biosynthetic potential for carotenoid accumulation in genetically diverse germplasm of maize. Plant Physiol. **150:** 562–572.

van Bokhoven, H., Verver, J., Wellink, J., and van Kammen, A. (1993). Protoplasts transiently expressing the 200K coding sequence of cowpea mosaic virus B-RNA support replication of M-RNA. J. Gen. Virol. **74:** 2233–2241.

Velayos, A., Eslava, A.P., and Iturriaga, E.A. (2000). A bifunctional enzyme with lycopene cyclase and phytoene synthase activities is encoded by the carRP gene of *Mucor circinelloides*. Eur. J. Biochem. **267:** 5509–5519.

Vermaas, W.F., Timlin, J.A., Jones, H.D., Sinclair, M.B., Nieman, L.T., Hamad, S.W., Melgaard, D.K., and Haaland, D.M. (2008). In vivo hyperspectral confocal fluorescence imaging to determine pigment localization and distribution in cyanobacterial cells. Proc. Natl. Acad. Sci. USA **105:** 4050–4055.

Vidi, P.-A., Kanwischer, M., Baginsky, S., Austin, J.R., Csucs, G., Dörmann, P., Kessler, F., and Bréhélin, C. (2006). Tocopherol cyclase (VTE1) localization and vitamin E accumulation in chloroplast plastoglobule lipoprotein particles. J. Biol. Chem. **281:** 11225–11234.

Vidi, P.-A., Kessler, F., and Bréhélin, C. (2007). Plastoglobules: A new address for targeting recombinant proteins in the chloroplast. BMC Biotechnol. **7:** 4.

Walter, M.H., Floss, D.S., and Strack, D. (2010). Apocarotenoids: Hormones, mycorrhizal metabolites and aroma volatiles. Planta **232:** 1–17.

Wang, L., Goodey, N.M., Benkovic, S.J., and Kohen, A. (2006). Coordinated effects of distal mutations on environmentally coupled tunneling in dihydrofolate reductase. Proc. Natl. Acad. Sci. USA **103:** 15753–15758.

Welsch, R., Arango, J., Bär, C., Salazar, B., Al-Babili, S., Beltrán, J., Chavarriaga, P., Ceballos, H., Tohme, J., and Beyer, P. (2010). Provitamin A accumulation in cassava (*Manihot esculenta*) roots driven by a single nucleotide polymorphism in a phytoene synthase gene. Plant Cell **22:** 3348–3356.

Welsch, R., Beyer, P., Hugueney, P., Kleinig, H., and von Lintig, J. (2000). Regulation and activation of phytoene synthase, a key enzyme in carotenoid biosynthesis, during photomorphogenesis. Planta **211:** 846–854.

Welsch, R., Wüst, F., Bär, C., Al-Babili, S., and Beyer, P. (2008). A third phytoene synthase is devoted to abiotic stress-induced abscisic acid formation in rice and defines functional diversification of phytoene synthase genes. Plant Physiol. **147:** 367–380.

Wrischer, M., Prebeg, T., Magnus, V., and Ljubesic, N. (2007). Crystals and fibrils in chromoplast plastoglobules of *Solanum capsicastrum* fruit. Acta Bot. Croat. **66:** 81–87.

Wurtzel, E.T. (2004). Genomics, genetics, and biochemistry of maize carotenoid biosynthesis. In Recent Advances in Phytochemistry, Vol. 38, J. Romeo, ed (New York: Elsevier Ltd.), pp. 85–110.

Wurtzel, E.T., Cuttriss, A., and Vallabhaneni, R. (2012). Maize provitamin a carotenoids, current resources, and future metabolic engineering challenges. Front. Plant Sci. **3:** 29.

Xu, X., et al; Potato Genome Sequencing Consortium (2011). Genome sequence and analysis of the tuber crop potato. Nature **475:** 189–195.

Yan, J., et al. (2010). Rare genetic variation at *Zea mays crtRB1* increases beta-carotene in maize grain. Nat. Genet. **42:** 322–327.

Ytterberg, A.J., Peltier, J.-B., and van Wijk, K.J. (2006). Protein profiling of plastoglobules in chloroplasts and chromoplasts. A surprising site for differential accumulation of metabolic enzymes. Plant Physiol. **140:** 984–997.

Zbierzak, A.M., Kanwischer, M., Wille, C., Vidi, P.A., Giavalisco, P., Lohmann, A., Briesen, I., Porfirova, S., Bréhélin, C., Kessler, F., and Dörmann, P. (2010). Intersection of the tocopherol and plastoquinol metabolic pathways at the plastoglobule. Biochem. J. **425:** 389–399.

Zhang, R., Wise, R.R., Struck, K.R., and Sharkey, T.D. (2010). Moderate heat stress of *Arabidopsis thaliana* leaves causes chloroplast swelling and plastoglobule formation. Photosynth. Res. **105:** 123–134.

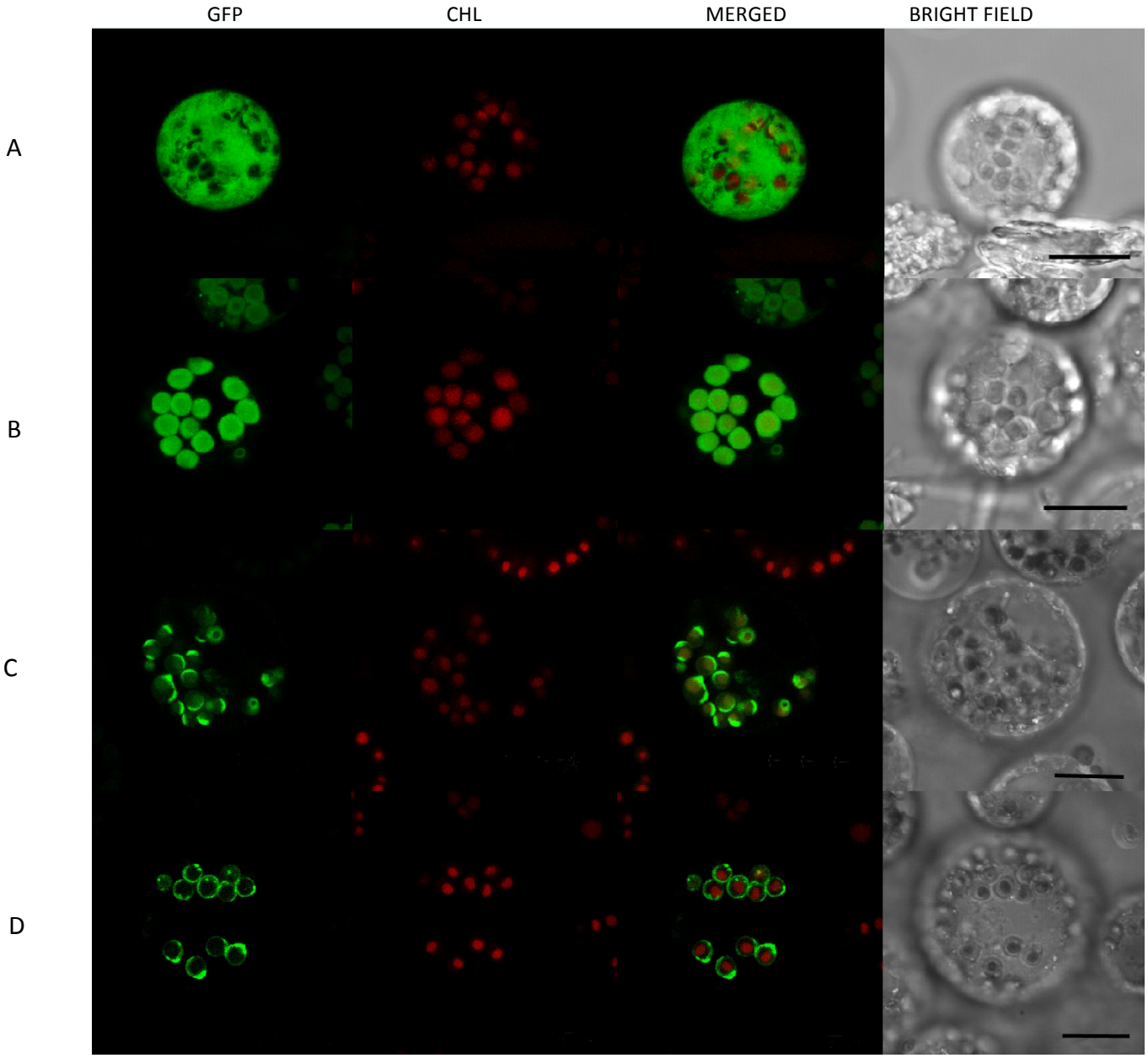

Supplemental Figure 1. Overexpression of proteins with known location in etiolated maize protoplasts. **A** – soluble GFP (protoplasts transformed with pUC35S-sGFP-Nos), GFP is localized to cell cytoplasm. **B**-LHCP-GFP (protoplasts transformed with pUC35S-LHCP-sGFP-Nos), LHCP is an integral protein from thylakoid membrane and colocalized with chlorophyll fluorescence. **C** – At-APG1 (protoplasts transformed with pFB70), **D** – At-Tic40 (protoplasts transformed with pFB71). At-APG1 and At-Tic40 are proteins from chloroplast inner envelope membrane (Breuers et al., 2012) and demonstrate half-moon or circle pattern correspondingly. **Chl** – chlorophyll autofluorescence. Bar = 10 μm.

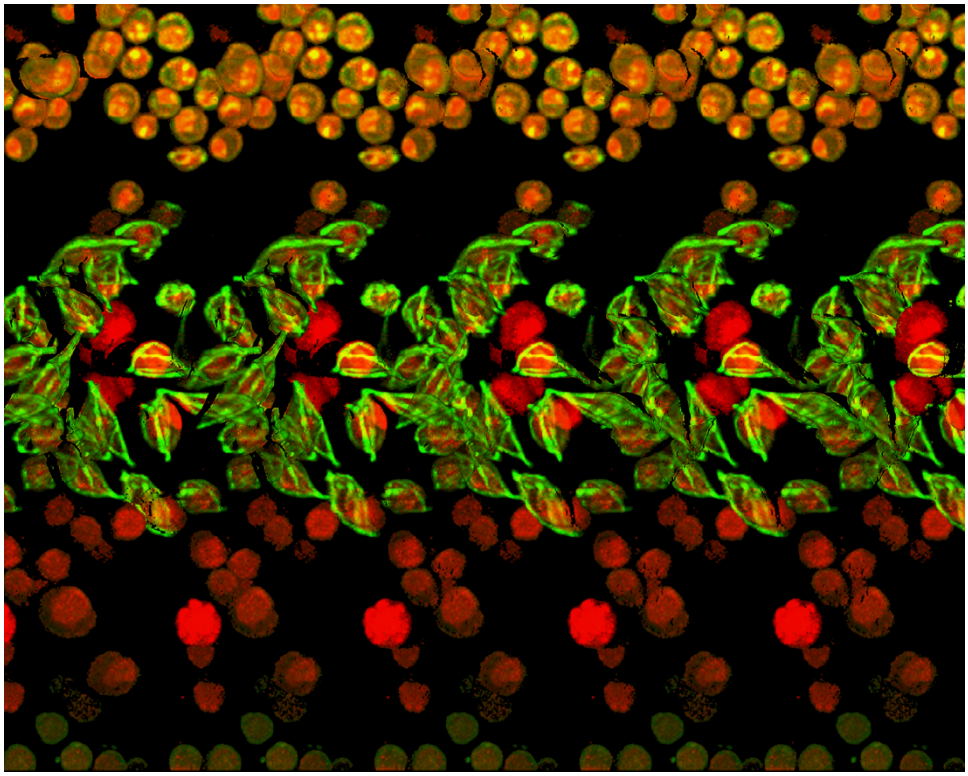

original:

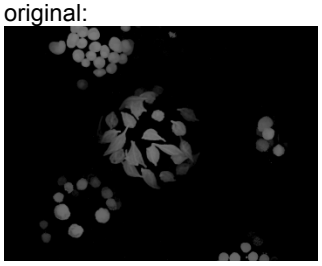

Supplemental Figure 2. Hidden 3D ("third eye") stereogram of transiently expressed Zm-PSY1-NP-GFP in etiolated maize protoplasts. Zm-PSY1-NP-GFP is forming characteristic spikes. Stereogram prepared from original microscopic image by Hidden 3D studio, USA. It can be viewed by unfocusing the eyes and looking "through" the image. Additional instructions for viewing 3-D sterograms can be found at: http://www.hidden-3d.com/how_to_view_stereogram.php.

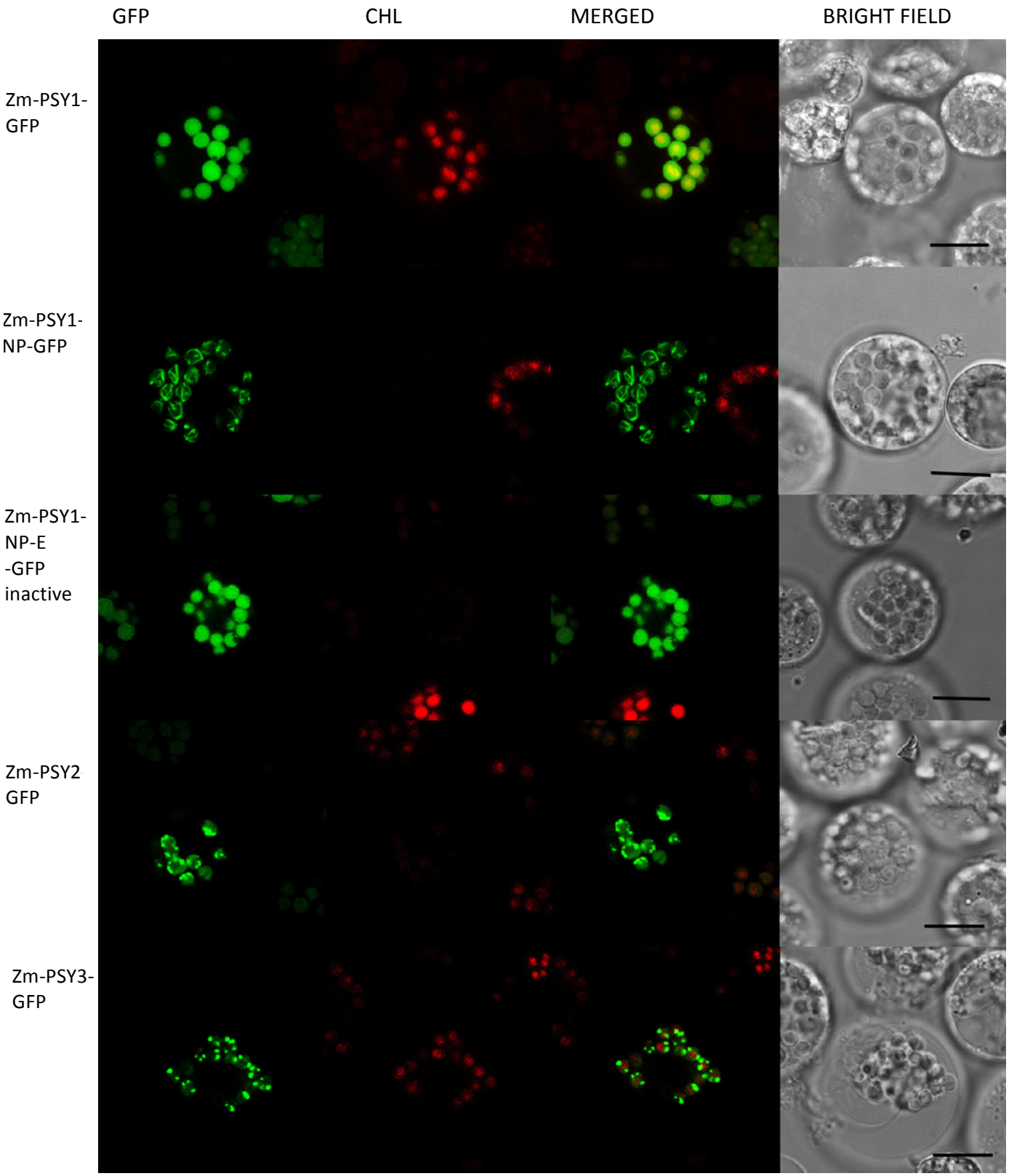

Supplemental Figure 3. Transient expression of Zm-PSY-GFP variants in etiolated maize protoplasts from PSY1 knockout line, *y1-8549*. The localization pattern is consistent with the one in protoplasts from standard B73 line.

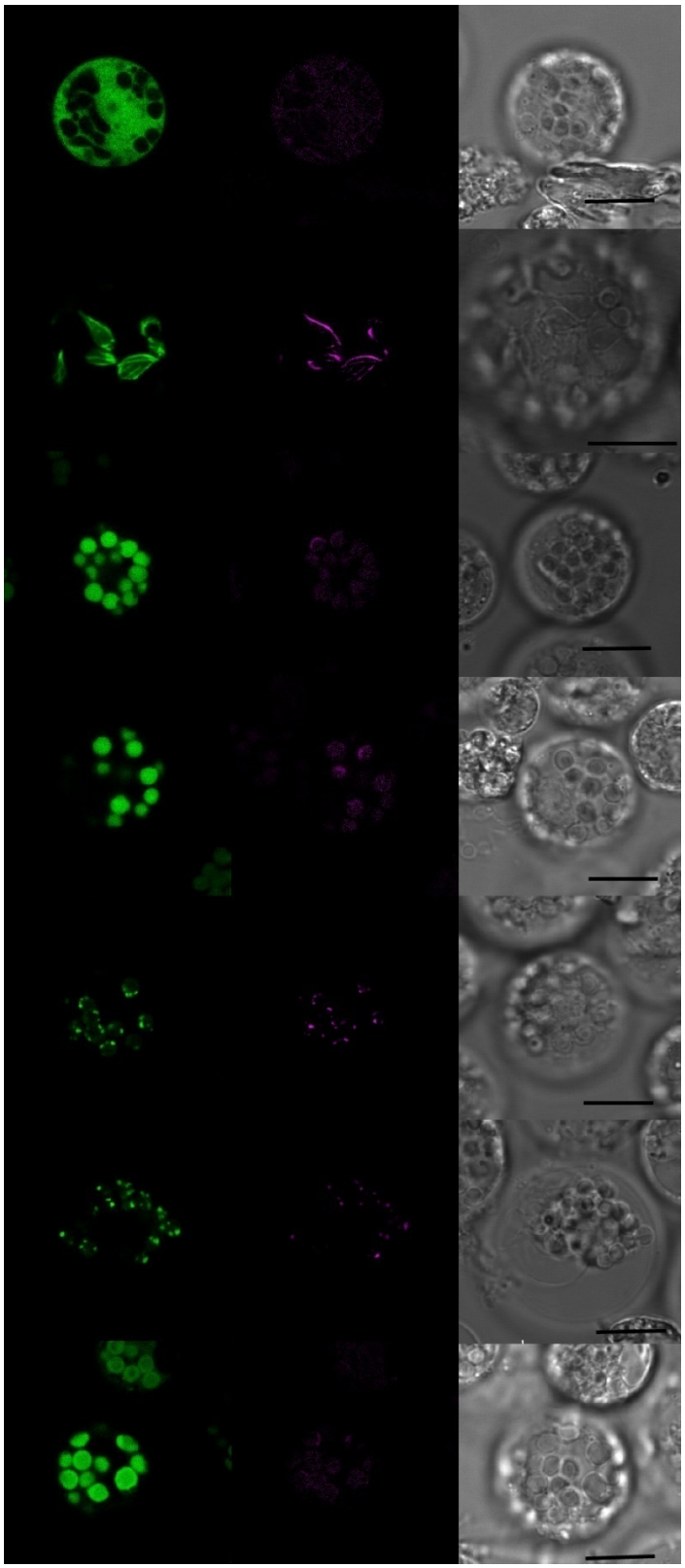

Supplemental Figure 4. Spectral dye separation for transiently expressed GFP-fusion proteins in maize PSY1 knockout leaf protoplasts. Different fusion protein constructs were transiently expressed in protoplasts, isolated from etiolated leaves of maize PSY1 knockout plants. GFP and carotenoid fluorescent spectra were separated using Spectral Dye Separation tool in LAS AF software (Leica Microsystems). Carotenoids have a low fluorescence emission between 500 and 650 nm which can be excited by a 488 nm laser (Vermaas et al., 2008). The software separates the carotenoid emission from the GFP emission. To eliminate any background carotenoid fluorescence in the absence of a PSY transgene, we used protoplasts prepared form Zm-PSY1-knockout maize *y1-8549* which are unable to produce carotenoids in the absence of the transgenically supplied PSY (Li et al, 2008b). Soluble cytoplasmic GFP, used as a negative control and GFP spectrum reference, showed no carotenoid emission (**A**). Fibrils formed by Zm-PSY1-NP (**B**) have bright fluorescence in the carotenoid channel suggesting presence of concentrated carotenoids. Such fluorescence disappeared, showing no fibrils when non-active Zm-PSY1-NP-E was overexpressed in etioplasts (**C**). A low level of carotenoid fluorescence was observed in etioplasts carrying overexpressed Zm-PSY1-NT (**D**) which might be due to a basal level of carotenoid biosynthesis in leaves due to inactivity of Zm-PSY when not attached to membranes (Schledz et al., 1996). Punctuated dots, formed in etioplasts by Zm-PSY2-GFP and Zm-PSY3-GFP (**E, F**), also show bright fluorescence in the carotenoid channel suggesting presence of concentrated carotenoids. In contrast, only background level of fluorescence is observed when a control chloroplast-localized noncarotenoid protein is introduced (integral thylakoid membrane protein LHCP (Tan et al., 2001) (**G**). **A** – soluble GFP without any protein or transit peptide attached, localized to protoplast cytoplasm; **B** – Zm-PSY1-NP-GFP; **C** – Zm-PSY1-NP-E-GFP; **D** – Zm-PSY1-NT-GFP; **E** – Zm-PSY2-GFP; **F** – Zm-PSY3-GFP; **G** – LHCP-GFP (negative control of plastid protein fused with GFP; LHCP is a not involved in carotenoid biosynthesis). **GFP, Carotenoids** – maximum projection of corresponding isolated fluorescent spectra; **Bright field** – bright field image of the protoplast. Bar = 10 μm.

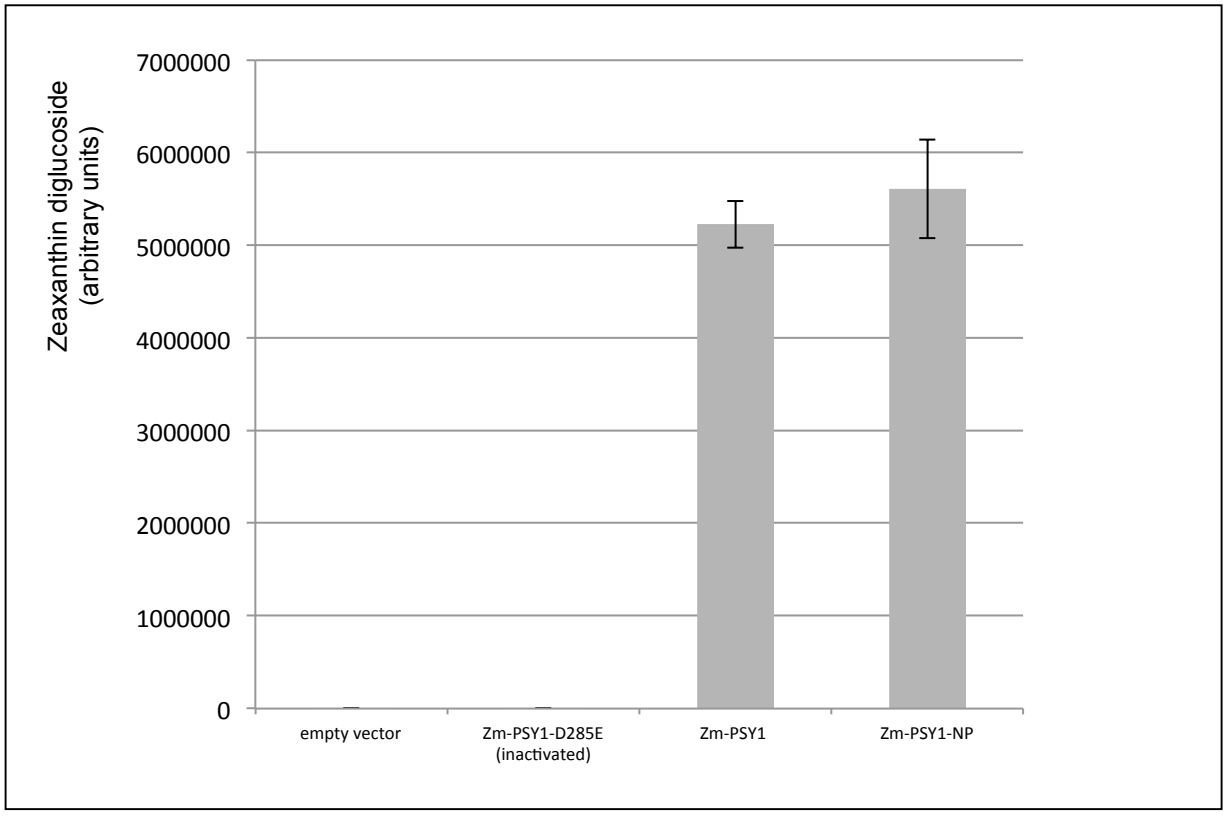

Supplemental Figure 5. *E. coli* complementation test. *E. coli* Top10 with pACCAR25ΔcrtB carrying carotenoid biosynthetic enzymes for zeaxanthin production, but lacking the PSY enzyme, was transformed with different mutagenized variants of Zm-PSY1. Active PSY enzymes were able to complement the pathway which resulted in zeaxanthin production. Zeaxanthin was extracted from pelleted cells by methanol and then analyzed by HPLC to detect the relative amount produced, which was calculated as peak area divided by OD of the *E. coli* culture. The experiment was repeated 3 times. Zm-PSY1, Zm-PSY1-NP were active in this test, Zm-PSY1-D_{285}E was inactive. Empty expression vector (pBluescript) was used as a negative control.

Supplemental Table 1. Plasmids generated and primers used for cloning

Plasmid	Primers used for cloning	Restriction sites used for cloning
pTnT-Zm-PSY1	F 5' TCTCGAGATGGCCATCATACTCGTACGAG R 5' ATCTAGACTAGGTCTGGCCATTTCTCAATG	XhoI/XbaI
pTnT-Zm-PSY2	F 5' ACTCGAGAATGGCTGCGGGCTCGTCCG R 5' GAT GTG ATC TAC GGA TGG TTC AT	XhoI/NotI
pTnT-Zm-PSY3	F 5' AAGAATTC*GCCACC*ATGATGTCTACGAGC R 5' AAGCGGCCGCCTATGTTAGGGTGGAATAGC	EcoRI+Kozak sequence, NotI
pUC35S-Zm-PSY1-sGFP-Nos	F 5' TTCTAGAATGGCCATCATACTCGTACGAG R 5' AGGATCCGGTCTGGCCATTTCTCAATGAA	XbaI/BamHI
pUC35S-Zm-PSY2-sGFP-Nos	F 5' ATCTAGAATGGCTGCGGGCTCGTCC R 5' AGGATCCTGGTGCAACCGCAGCCCTTGCA	XbaI/BamHI
pUC35S-Zm-PSY3-sGFP-Nos	F 5' ATCTCTAGAATGATGTCTACGAGCCGCGCGGTGAAGTCG R 5' ATCGGATCCTGTTAGGGTGGAATAGCGTCTCCGGCTC	XbaI/BamHI
pUC35S-Os-PSY1-sGFP-Nos	F 5'ATCTAGAATGGCCCATCACGCTCCTAC R 5'A AGATCTCTTCTGGCT ATT TCT CAG TGA G	XbaI/BglI
pUC35S-Os-PSY2-sGFP-Nos	F 5'AAC TAGTTCCACACGAACACACAACCCCAA R 5' AAGATCTTGATGCAACTGCCGCTCTTGCATA	SpeI/BglI
pUC35S-Os-PSY3-sGFP-Nos	F 5' ATCGTCTAGAATGATGTCCACCACCACCACC R 5' ATCGGGATCCTGATGATGTTAGGCTAGAGC	XbaI/BamHI
pUC35S-LHCP-sGFP-Nos	F 5' ATCTCTAGAATGGCCGCTTCATCC R 5' ATCGGATCCCTTTCCGGGAACAAAGTTGGTAGC	XbaI/BamHI
pSAT-At-PSY-RFP	F 5' ATCGAATTCATGTCTTCTTCTGTAGCAGTG R 5' ATTGGATCCGTATCGATAGTCTTGAACTTG	EcoRI/BamHI
pSAT-Zm-PG2-RFP	F 5' ATCGAATTCATGGCGTCCTCCGCGTTCCTCAACG R 5' ATCTGATCAGGTATAGAAGAGTACTTCCC	EcoRI/BclI
pUC35S-Zm-PSY1-NP-sGFP-Nos	F 5' CCTGTGATGGGCATCGCACCCGAGTCTAAAG R 5' CTTTAGACTCGGGTGCGATGCCCATCACAGG	-
pUC35S-Zm-PSY1-SP-sGFP-Nos	F 5' CCTGTGATGGGCATCGCACCCGAGTCTAAAG R 5' CTTTAGACTCGGGTGCGATGCCCATCACAGG F 5' GATGGGCCAAACGCCAGCTACATTACACCAACAG R 5'CTGTTGGTGTAATGTAGCTGGCGTTTGGCCCATC	-
pUC35S-Zm-PSY1-NS-sGFP-Nos	F 5' CCTGTGATGGGCATCGCATCCGAGTCTAAAG R 5' CTTTAGACTCGGATGCGATGCCCATCACAGG	-
pUC35S-Zm-PSY1-ST-sGFP-Nos	F 5' GATGGGCCAAACGCCAGCTACATTACACCAACAG R 5' CTGTTGGTGTAATGTAGCTGGCGTTTGGCCCATC	-
pUC35S-Zm-PSY2-ST-sGFP-Nos	F 5' CCTGTCATGGGCATCGCTACCGACTCCAA R 5' TTGGAGTCGGTAGCGATGCCCATGACAGG	-
pUC35S-Zm-PSY2-NT-sGFP-Nos	F 5' CCTGTCATGGGCATCGCTACCGACTCCAA R 5' TTGGAGTCGGTAGCGATGCCCATGACAGG F 5' GACGGTCCCAACGCGAACTACATCACGCCGAC R 5' GTCGGCGTGATGTAGTTCGCGTTGGGACCGTC	-
pSAT-Zm-PSY2-NP- RFP	F 5' GACGGTCCCAACGCGAACTACATCACGCCGAC R 5' GTCGGCGTGATGTAGTTCGCGTTGGGACCGTC	-
pUC35S-Os-PSY1-NT-sGFP-Nos	F 5' GTTCCTGTGATGGGTATTGCAACCGAGTCGAAG R 5' 5' CTTCGACTCGGTTGCAATACCCATCACAGGAAC	-
pBS-Zm-PSY1-NP	F 5' CCTGTGATGGGCATCGCACCCGAGTCTAAAG R 5' CTTTAGACTCGGGTGCGATGCCCATCACAGG	-
pBS-Zm-PSY1-D_{285}E	F 5' CGAACATACTCCGGGAGGTTGGAGAGGATGCTA R 5' TAGCATCCTCTCCAACCTCCCGGAGTATGTTCG	-

pUC35S-Zm-PSY1-NP-E-sGFP-Nos	F 5′ CGAACATACTCCGGGAGGTTGGAGAGGATGCTA R 5′ TAGCATCCTCTCCAACCTCCCGGAGTATGTTCG F 5′ CCTGTGATGGGCATCGCACCCGAGTCTAAAG R 5′ CTTTAGACTCGGGTGCGATGCCCATCACAGG	-

Supplemental References:

Breuers, F.K.H., Braeutigam, A., Geimer, S., Welzel, U.Y., Stefano, G., Renna, L., Brandizzi, F., and Weber, A.P.M. (2012). Dynamic remodeling of the plastid envelope membranes - a tool for chloroplast envelope *in vivo* localizations. Frontiers in Plant Science **3**.

Li, F., Vallabhaneni, R., Yu, J., Rocheford, T., and Wurtzel, E.T. (2008b). The maize phytoene synthase gene family: overlapping roles for carotenogenesis in endosperm, photomorphogenesis, and thermal stress-tolerance. Plant Physiol. **147,** 1334-1346.

Schledz, M., Al-Babili, S., von Lintig, J., Haubruck, H., Rabbani, S., Kleinig, H., and Beyer, P. (1996). Phytoene synthase from *Narcissus pseudonarcissus*: functional expression, galactolipid requirement, topological distribution in chromoplasts and induction during flowering. Plant J **10,** 781-792.

Tan, B.C., Cline, K., and McCarty, D.R. (2001). Localization and targeting of the VP14 epoxy-carotenoid dioxygenase to chloroplast membranes. Plant J **27,** 373-382.

Vermaas, W.F., Timlin, J.A., Jones, H.D., Sinclair, M.B., Nieman, L.T., Hamad, S.W., Melgaard, D.K., and Haaland, D.M. (2008). In vivo hyperspectral confocal fluorescence imaging to determine pigment localization and distribution in cyanobacterial cells. Proceedings of the National Academy of Sciences of the United States of America **105,** 4050-4055.